Appendix A
Fierz Transformations

Fierz identities are often considered in the context of particular relationships between pairs of fermion bilinears—probably the most well known is

$$(\gamma^{\mu} P_L)_{ij} (\gamma_{\mu} P_L)_{kl} = -(\gamma^{\mu} P_L)_{il} (\gamma_{\nu} P_L)_{kj}$$

which is often useful in flavour physics calculations and also in e.g. the calculation of the MSW [1, 2] effect for neutrino propagation in matter.

However they can instead be considered (perhaps more correctly) as a set of identities that can be found for any complete set of square matrices, which arise simply as a consequence of completeness relations over this basis set.

In general, if we have some matrix vector space which is spanned by the basis set $\{M^i\}$, then we can write identities of the form

$$M^i \otimes M^j = M^k \otimes M^l \,.$$

In this way, the colour rearrangement identity

$$t^a_{ij} t^a_{kl} = \frac{1}{2} \left(\delta_{il} \delta_{kj} - \frac{1}{N_c} \delta_{ij} \delta_{kl} \right) \tag{A.0.1}$$

can be viewed as a Fierz identity, since the space of 3×3 matrices is spanned by the set $\{t^a\}$ of generators of $SU(3)$ plus the identity matrix.

A useful introduction to generalised Fierz identities and how to calculate them is [3]. We will use the notation of that paper (itself taken from Takahashi [4]) in the rest of this appendix, where we list some identities that are used in this thesis. It is important to note that when these identities are used in conjunction with fermionic operators rather than spinors, an extra minus sign will arise from the anti-commuting nature of the operators.

$$(\gamma^{\mu} P_L)[\gamma_{\mu} P_L] = -(\gamma^{\mu} P_L][\gamma_{\mu} P_L) \tag{A.0.2}$$

M. J. Kirk, *Charming New Physics in Beautiful Processes?*,
Springer Theses, https://doi.org/10.1007/978-3-030-19197-9

$$(\gamma^{\mu}\gamma^{\nu}\gamma^{\lambda}P_L)[\gamma_{\lambda}\gamma_{\nu}\gamma_{\mu}P_L] = -4(\gamma^{\mu}P_L][\gamma_{\mu}P_L) \tag{A.0.3}$$

$$(P_L)[P_L] = \frac{1}{2}(P_L][P_L) + \frac{1}{8}(\sigma^{\mu\nu}P_L][\sigma_{\mu\nu}P_L) \tag{A.0.4}$$

$$(P_L)[P_R] = \frac{1}{2}(\gamma^{\mu}P_R][\gamma_{\mu}P_L) \tag{A.0.5}$$

$$(\sigma_{\mu\nu}P_L)[\sigma^{\mu\nu}P_L] = 6(P_L][P_L) - \frac{1}{2}(\sigma^{\mu\nu}P_L][\sigma_{\mu\nu}P_L) \tag{A.0.6}$$

$$(\sigma_{\mu\nu}P_L)[\sigma^{\mu\nu}P_R] = 0 \tag{A.0.7}$$

$$(\sigma_{\alpha\beta}\sigma_{\mu\nu}P_L)[\sigma^{\mu\nu}\sigma^{\alpha\beta}P_L] = 72(P_L][P_L) + 2(\sigma^{\mu\nu}P_L][\sigma_{\mu\nu}P_L) \tag{A.0.8}$$

References

1. Mikheyev SP, Smirnov A Yu (1985) Resonance amplification of oscillations in matter and spectroscopy of solar neutrinos. Sov J Nucl Phys 42:913–917
2. Wolfenstein L (1978) Neutrino oscillations in matter. Phys Rev D 17:2369–2374. https://doi.org/10.1103/PhysRevD.17.2369
3. Nishi CC (2005) Simple derivation of general Fierz-like identities. Am J Phys 73:1160–1163. https://doi.org/10.1119/1.2074087, arXiv:hep-ph/0412245
4. Takahashi Y (1986) The Fierz identities. In: Ezawa H, Kamefuchi S (eds) Progress in quantum field theory. North-Holland, pp 121–132

Appendix B
Feynman Rules

Our SM Feynman rules can be found by taking those in [1] and setting $\eta = \eta_s = \eta' = \eta_e = -1$ and $\eta_Z = \eta_\theta = \eta_Y = 1$. (Note that in that work all particles are considered incoming in Feynman diagrams.) These match the conventions of [2].

In Table B.1, we show the Feynman rules for heavy quarks in HQET.

M. J. Kirk, *Charming New Physics in Beautiful Processes?*,
Springer Theses, https://doi.org/10.1007/978-3-030-19197-9

Table B.1 HQET Feynman rules

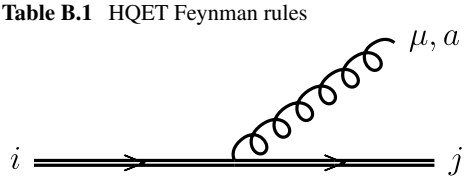

$$\sim ig_s v^\mu t^a_{ji}$$

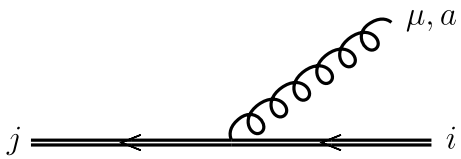

$$\sim -ig_s v^\mu t^a_{ji}$$

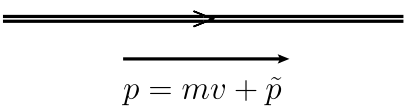

$$\sim \frac{i(\mathbb{1}+\not{v})}{2v\cdot\tilde{p}}$$

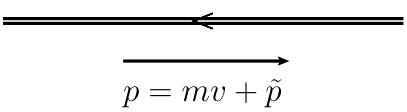

$$\sim \frac{i(\mathbb{1}-\not{v})}{2v\cdot\tilde{p}}$$

References

1. Romao JC, Silva JP (2012) A resource for signs and Feynman diagrams of the standard model. Int J Mod Phys A 27:1230025. https://doi.org/10.1142/S0217751X12300256, arXiv:1209.6213
2. Peskin ME, Schroeder DV (1995) An introduction to quantum field theory. Addison-Wesley, Reading, USA

Appendix C
Four Quark Matrix Elements

In phenomenological calculations matrix elements of four quark operators often arise, and so knowing these matrix elements is of vital importance to being able to make theoretical predictions. However these are non-perturbative objects and so calculating them is non-trivial. Nowadays, lattice QCD has progressed to the point of being able to provide precision determinations, but historically other techniques were used. In particular the Vacuum Saturation Approximation (VSA) is a simple way of analytically approximating the result, and current data shows it even holds numerically at the 10–20% level [1, 2]. The VSA approximates the four quark matrix elements as a product of decay to vacuum operators, and so gives us an estimate in terms of meson decay constants plus various colour factors. Below we show an example of a VSA calculation, and then we list the results for different operators.

Note that we show results in this appendix for B_s–$\bar{B}_s$ mixing and B_s lifetime calculations—the generalisation to B_d, D, etc. mesons can be found by making the obvious substitutions.

VSA Calculation Example

If we take the operator $\mathcal{O}_1 = (\bar{b}^i \gamma_\mu P_L s^i)(\bar{b}^j \gamma^\mu P_L s^j)$, there are four ways to contract this with an incoming B_s and outgoing $\bar{B}_s$ state—two for the b quarks and two for the s quarks. Making use of the Fierz identities stated in Eqs. A.0.1 and A.0.2, we can write the matrix element $\langle \bar{B}_s | \mathcal{O}_1 | B_s \rangle \equiv \langle \mathcal{O}_1 \rangle$ as

$$\begin{aligned}
\langle \mathcal{O}_1 \rangle &= \langle \bar{B}_s | (\bar{b}^i \gamma^\mu P_L s^i)(\bar{b}^j \gamma_\mu P_L s^j) | B_s \rangle \\
&= 2 \Big[\quad \Big(\langle \bar{B}_s | \bar{b}^i \gamma^\mu P_L s^i \Big) \Big(\bar{b}^j \gamma_\mu P_L s^j | B_s \rangle \Big) \\
&\qquad + \Big(\langle \bar{B}_s | \bar{b}^i \gamma^\mu P_L s^j \Big) \Big(\bar{b}^j \gamma_\mu P_L s^i | B_s \rangle \Big) \Big] \\
&= 2 \Big[\Big(1 + \frac{1}{N_c} \Big) \Big(\langle \bar{B}_s | \bar{b}^i \gamma^\mu P_L s^i \Big) \Big(\bar{b}^j \gamma_\mu P_L s^j | B_s \rangle \Big) \\
&\qquad\qquad + 2 \Big(\langle \bar{B}_s | \bar{b}^i \gamma^\mu P_L t^a_{ij} s^j \Big) \Big(\bar{b}^k \gamma_\mu P_L t^a_{kl} s^l | B_s \rangle \Big) \Big],
\end{aligned}$$

M. J. Kirk, *Charming New Physics in Beautiful Processes?*,
Springer Theses, https://doi.org/10.1007/978-3-030-19197-9

where the round brackets fix the operator contraction. (The factor of two is the same as seen in Eq. 2.4.18.) We then take the completeness relation $I = \sum_X |X\rangle\langle X|$ and insert it into the middle of the four quark operator:

$$\langle \mathcal{O}_1 \rangle = 2 \sum_X \Big[\left(1 + \frac{1}{N_c}\right) \langle \bar{B}_s | \bar{b}^i \gamma^\mu P_L s^i | X \rangle \langle X | \bar{b}^j \gamma_\mu P_L s^j | B_s \rangle + 2 \langle \bar{B}_s | \bar{b}^i \gamma^\mu P_L t^a_{ij} s^j | X \rangle \langle X | \bar{b}^k \gamma_\mu P_L t^a_{kl} s^l | B_s \rangle \Big] .$$

The VSA amounts to assuming the vacuum state dominates this sum, and so we can write

$$\langle \mathcal{O}_1 \rangle \overset{\text{VSA}}{=} 2 \Big[\left(1 + \frac{1}{N_c}\right) \langle \bar{B}_s | \bar{b}^i \gamma^\mu P_L s^i | 0 \rangle \langle 0 | \bar{b}^j \gamma_\mu P_L s^j | B_s \rangle + 2 \langle \bar{B}_s | \bar{b}^i \gamma^\mu P_L t^a_{ij} s^j | 0 \rangle \langle 0 | \bar{b}^k \gamma_\mu P_L t^a_{kl} s^l | B_s \rangle \Big] .$$

The second term goes to zero as the colour octet operator cannot annihilate a colour singlet meson, while for the first term we can use the definitions of the meson decay constant

$$\left. \begin{aligned} \langle 0 | \bar{b} \gamma_\mu s | B_s(p) \rangle &= 0 \\ \langle 0 | \bar{b} \gamma_\mu \gamma^5 s | B_s(p) \rangle &= i p_\mu f_{B_s} \end{aligned} \right\} \Rightarrow \langle 0 | \bar{b} \gamma_\mu P_{L,R} s | B_s(p) \rangle = \mp \frac{i}{2} p_\mu f_{B_s} \qquad \text{(C.0.1)}$$

to give our result

$$\begin{aligned} \langle \mathcal{O}_1 \rangle &\overset{\text{VSA}}{=} 2 \left(1 + \frac{1}{N_c}\right) \left(-\frac{i}{2} p^\mu f_{B_s}\right)^\dagger \left(-\frac{i}{2} p_\mu f_{B_s}\right) \\ &= \frac{1}{2} \left(1 + \frac{1}{N_c}\right) M^2_{B_s} f^2_{B_s} . \end{aligned}$$

Since the VSA is only an approximation, we introduce an extra correction factor, known as the bag parameter,[1] to account for deviations from this behaviour and write the matrix element as

$$\langle \bar{B}_s | \mathcal{O}_1 | B_s \rangle = \frac{2}{3} f^2_{B_s} M^2_{B_s} B_1 .$$

ΔF= 2 Operators

For $\Delta F = 2$ operators, we can use Fierz relations to reduce the set of possible dimension-six operators which can arise to a minimal basis set, which are shown below:

[1] The term "bag" dates back to the MIT bag model of hadrons.

$$
\begin{aligned}
\mathcal{O}_1 &= (\bar{b}^\alpha \gamma^\mu P_L s^\alpha)(\bar{b}^\beta \gamma_\mu P_L s^\beta)\,, \\
\mathcal{O}_2 &= (\bar{b}^\alpha P_L s^\alpha)(\bar{b}^\beta P_L s^\beta)\,, \\
\mathcal{O}_3 &= (\bar{b}^\alpha P_L s^\beta)(\bar{b}^\beta P_L s^\alpha)\,, \\
\mathcal{O}_4 &= (\bar{b}^\alpha P_L s^\alpha)(\bar{b}^\beta P_R s^\beta)\,, \\
\mathcal{O}_5 &= (\bar{b}^\alpha P_L s^\beta)(\bar{b}^\beta P_R s^\alpha)\,, \\
\widetilde{\mathcal{O}}_1 &= (\bar{b}^\alpha \gamma^\mu P_R s^\alpha)(\bar{b}^\beta \gamma_\mu P_R s^\beta)\,, \\
\widetilde{\mathcal{O}}_2 &= (\bar{b}^\alpha P_R s^\alpha)(\bar{b}^\beta P_R s^\beta)\,, \\
\widetilde{\mathcal{O}}_3 &= (\bar{b}^\alpha P_R s^\beta)(\bar{b}^\beta P_R s^\alpha)\,.
\end{aligned}
$$

This minimal set was first derived in the context of supersymmetric extensions of the SM [3], and so is often referred to as the "SUSY basis". Since parity is a symmetry of QCD, $\langle\widetilde{\mathcal{O}}\rangle = \langle\mathcal{O}\rangle$ holds as long as we don't consider electroweak corrections to the matrix elements. At dimension seven, there are several more operators that arise—see [4] for details.

The matrix elements of the SUSY basis can be written in the form (notation taken from [5])

$$
\begin{aligned}
\langle\mathcal{O}_1\rangle &= c_1 f_{B_s}^2 M_{B_s}^2 B_1\,, \\
\langle\mathcal{O}_i\rangle &= c_i f_{B_s}^2 M_{B_s}^2 \left(\frac{M_{B_s}}{m_b + m_s}\right)^2 B_i \quad (i = 2, 3)\,, \\
\langle\mathcal{O}_i\rangle &= c_i f_{B_s}^2 M_{B_s}^2 \left[\left(\frac{M_{B_s}}{m_b + m_s}\right)^2 + d_i\right] B_i \quad (i = 4, 5)\,,
\end{aligned}
\tag{C.0.2}
$$

where $c_i = \{{}^2\!/_3, -{}^5\!/_{12}, {}^1\!/_{12}, {}^1\!/_2, {}^1\!/_6\}$, $d_4 = {}^1\!/_6$, and $d_5 = {}^3\!/_2$. These prefactors can be derived in the same way as in the above example, making use of Eqs. A.0.4 and A.0.5, as well as the following two further relations involving the decay constant. We can show

$$\langle 0|\bar{b} P_{L,R} s|B_s(p)\rangle = \pm\frac{i}{2}\frac{M_{B_s}}{m_b + m_s} f_{B_s}$$

by contracting the meson momentum p^μ with our result in Eq. C.0.1 (see Sect. 4 of [6]); we must also have

$$\langle 0|\bar{b}\sigma^{\mu\nu} s|B_s(p)\rangle = 0$$

since we cannot construct an antisymmetric Lorentz tensor out of a single 4-momentum.

ΔF= 0 Operators

For $\Delta F = 0$ operators, the standard set considered (which are those which arise in the SM) is

$$\begin{aligned} Q_1 &= (\bar{b}\gamma^\mu P_L q)(\bar{q}\gamma_\mu P_L b) \\ Q_2 &= (\bar{b} P_L q)(\bar{q} P_L b) \\ T_1 &= (\bar{b}\gamma^\mu t^a P_L q)(\bar{q}\gamma_\mu t^a P_L b) \\ T_2 &= (\bar{b} t^a P_L q)(\bar{q} t^a P_L b) \end{aligned}$$

which have matrix elements

$$\begin{aligned} \langle Q_i \rangle &= A_i f_{B_s}^2 M_{B_s}^2 B_i \\ \langle T_i \rangle &= A_i f_{B_s}^2 M_{B_s}^2 \epsilon_i \end{aligned} \tag{C.0.3}$$

where $B_i = 1$ and $\epsilon_i = 0$ in the VSA and

$$A_1 = \frac{1}{4}, \quad A_2 = \frac{1}{4}\left(\frac{M_{B_s}}{m_b + m_s}\right)^2. \tag{C.0.4}$$

References

1. Aoki S et al (2017) Review of lattice results concerning low-energy particle physics. Eur Phys J C 77:112. https://doi.org/10.1140/epjc/s10052-016-4509-7, arXiv:1607.00299
2. FLAG collaboration. http://flag.unibe.ch/MainPage
3. Gabbiani F, Gabrielli E, Masiero A, Silvestrini L (1996) A Complete analysis of FCNC and CP constraints in general SUSY extensions of the standard model. Nucl Phys B 477:321–352. https://doi.org/10.1016/0550-3213(96)00390-2, arXiv:hep-ph/9604387
4. Beneke M, Buchalla G, Dunietz I (1996) Width difference in the $B_s - \bar{B}_s$ system. Phys Rev D 54:4419–4431. https://doi.org/10.1103/PhysRevD.54.4419, https://doi.org/10.1103/PhysRevD.83.119902, arXiv:hep-ph/9605259
5. Fermilab Lattice, MILC collaboration, Bazavov A et al (2016) $B^0_{(s)}$-mixing matrix elements from lattice QCD for the standard model and beyond. Phys. Rev. D 93:113016. https://doi.org/10.1103/PhysRevD.93.113016, arXiv:1602.03560
6. Tanedo P (2009) One-Loop MSSM predictions for $B_{s,d} \to \ell^+\ell^-$ at low tan β, Master's thesis, Durham University. http://etheses.dur.ac.uk/2040/. (See also https://www.physics.uci.edu/~tanedo/files/documents/TanedoMSc.pdf for a non-scanned version)

Appendix D
Additional Information from "Quark-Hadron Duality"

In this appendix we present more information on the work in Chap. 3.

In Table D.1, we show the error breakdown for our updated lifetime ratio calculation in Eq. 3.2.32, which has an error smaller than the current experimental measurement by a factor of four, and the previous SM calculation by a factor two.

In Table D.2, we present the inputs for our "aggressive" SM calculation in Sect. 3.3.

In Tables D.3, D.4, D.5, D.6, D.7, D.8, D.9 and D.10 we present the error breakdown for our updated predictions.

Finally in Appendix D.2 we show the proof of the inequality used in Sect. 3.4.

D.1 Inputs and Detailed View of Uncertainties

Table D.1 Error breakdown for the SM prediction for $\tau(B_s)/\tau(B_d)$ given in Eq. 3.2.32

Parameter	Error contribution (%)
$\delta(\epsilon_1)$	0.0710
$\delta(\epsilon_2)$	0.0510
$\delta(f_{B_s})$	0.0290
$\delta(\mu_G^2(B_s)/\mu_G^2(B_d))$	0.0280
$\mu_\pi^2(B_s) - \mu_\pi^2(B_d))$	0.0230
$\delta(f_{B_d})$	0.0230
$\delta(c_3)$	0.0230
$\delta(\mu)$	0.0160
$\delta(B_1)$	0.0140
$\delta(\mu_G^2(B_d))$	0.0130

(continued)

M. J. Kirk, *Charming New Physics in Beautiful Processes?*,
Springer Theses, https://doi.org/10.1007/978-3-030-19197-9

Table D.1 (continued)

Parameter	Error contribution (%)
$\delta(B_2)$	0.0100
$\delta(c_G)$	0.007
$\delta(m_b)$	0.004
$\delta(\lvert V_{cb}\rvert)$	0.003
$\delta(m_c)$	0.001
$\delta(\tau_{B_s})$	<0.001
$\delta(M_{B_s})$	<0.001
$\delta(M_{B_d})$	<0.001
$\delta(\lvert V_{us}\rvert)$	<0.001
$\delta(\gamma)$	<0.001
$\delta(\lvert V_{ub}/V_{cb}\rvert)$	<0.001
$\sum\delta$	0.108

Table D.2 Input parameters used in the "aggressive" determination of Sect. 3.3, compared to the previous SM calculation

Parameter	This work	ABL 2015 [1]
$f_{B_s}\sqrt{B}$	(0.223 ± 0.007) GeV	(0.215 ± 0.015) GeV
$f_{B_d}\sqrt{B}$	(0.185 ± 0.008) GeV	(0.175 ± 0.012) GeV
$B_3/B\ (B_s)$	1.15 ± 0.16	1.07 ± 0.06
$B_3/B\ (B_d)$	1.17 ± 0.24	1.04 ± 0.12
$\tilde{B}_{R_0}/B\ (B_s)$	0.54 ± 0.55	1.00 ± 0.3
$\tilde{B}_{R_0}/B\ (B_d)$	0.35 ± 0.80	1.00 ± 0.3
$\tilde{B}_{R_1}/B\ (B_s)$	1.61 ± 0.10	1.71 ± 0.26
$\tilde{B}_{R_1}/B\ (B_d)$	1.72 ± 0.15	1.71 ± 0.26
$\tilde{B}_{\tilde{R}_1}/B\ (B_s)$	1.223 ± 0.093	1.27 ± 0.16
$\tilde{B}_{\tilde{R}_1}/B\ (B_d)$	1.31 ± 0.14	1.27 ± 0.16
$\lvert V_{cb}\rvert$	$0.04180^{+0.00033}_{-0.00068}$	$0.04117^{+0.00090}_{-0.00114}$
$\lvert V_{ub}/V_{cb}\rvert$	0.0889 ± 0.0019	0.0862 ± 0.0044
γ	$1.170^{+0.015}_{-0.035}$	$1.171^{+0.017}_{-0.038}$
$\lvert V_{us}\rvert$	$0.22542^{+0.00042}_{-0.00031}$	$0.22548^{+0.00068}_{-0.00034}$

Table D.3 Error breakdown for the mass difference ΔM_s

Parameter	Error contribution	
	This work (%)	ABL 2015 [1] (%)
$\delta(f_{B_s}\sqrt{B})$	0.0635	0.139
$\delta(\lvert V_{cb}\rvert)$	0.0240	0.049
$\delta(m_t)$	0.0066	0.007
$\delta(\Lambda_{QCD})$	0.0013	0.001
$\delta(\gamma)$	0.0009	0.001
$\delta(m_b)$	0.0005	<0.001
$\delta(\lvert V_{ub}/V_{cb}\rvert)$	0.0004	0.001
$\sum\delta$	0.0682	0.148

Table D.4 Error breakdown for the mass difference ΔM_d

Parameter	Error contribution	
	This work (%)	ABL 2015 [1] (%)
$\delta(f_{B_d}\sqrt{B})$	0.0872	0.137
$\delta(\lvert V_{cb}\rvert)$	0.0240	0.049
$\delta(m_t)$	0.0066	0.001
$\delta(\Lambda_{QCD})$	0.0013	0.0
$\delta(\gamma)$	0.0208	0.002
$\delta(m_b)$	0.0005	0.0
$\delta(\lvert V_{ub}/V_{cb}\rvert)$	0.0001	0.0
$\sum\delta$	0.0931	0.148

Table D.5 Error breakdown for the width difference $\Delta\Gamma_s$

Parameter	Error contribution	
	This work (%)	ABL 2015 [1] (%)
$\delta(\mu)$	0.0889	0.084
$\delta(f_{B_s})$	0.0635	0.139
$\delta(B_{R_2})$	0.0604	0.148
$\delta(B_3)$	0.0539	0.021
$\delta(B_{R_0})$	0.0301	0.021
$\delta(\lvert V_{cb}\rvert)$	0.0240	0.049
$\delta(\bar{z})$	0.0109	0.011
$\delta(m_b)$	0.0080	0.008
$\delta(B_{\tilde{R}_1})$	0.0038	0.007
$\delta(m_s)$	0.0024	0.001
$\delta(B_{R_3})$	0.0023	0.002
$\delta(B_{R_1})$	0.0018	0.005
$\delta(\gamma)$	0.0010	0.001
$\delta(\Lambda_{QCD})$	0.0010	0.001
$\delta(\lvert V_{ub}/V_{cb}\rvert)$	0.0004	0.001
$\delta(m_t)$	0	<0.001
$\sum\delta$	0.1421	0.228

Table D.6 Error breakdown for the width difference $\Delta\Gamma_d$

Parameter	Error contribution	
	This work (%)	ABL 2015 [1] (%)
$\delta(\mu)$	0.0929	0.079
$\delta(f_{B_d})$	0.0872	0.137
$\delta(B_3)$	0.0809	0.04
$\delta(B_{R_2})$	0.0623	0.144
$\delta(B_{R_0})$	0.0533	0.025
$\delta(\lvert V_{cb}\rvert)$	0.0240	0.049
$\delta(\gamma)$	0.0233	0.002
$\delta(\bar{z})$	0.0109	0.011
$\delta(m_b)$	0.0076	0.008
$\delta(B_{R_3})$	0.0023	0.005
$\delta(\Lambda_{QCD})$	0.0009	0.001
$\delta(\lvert V_{ub}/V_{cb}\rvert)$	0.0008	0.001
$\delta(B_{\tilde{R}_1})$	0.0	0.0
$\delta(m_d)$	—	—
$\delta(B_{R_1})$	0.0	0.0
$\sum\delta$	0.175	0.227

Table D.7 Error breakdown for the ratio $\Delta\Gamma_s/\Delta M_s$

Parameter	Error contribution (%)
$\delta(\mu)$	0.0889
$\delta(B_{R_2})$	0.0604
$\delta(B_3)$	0.0539
$\delta(B_{R_0})$	0.0301
$\delta(\bar{z})$	0.0109
$\delta(m_b)$	0.0080
$\delta(m_t)$	0.0066
$\delta(\tilde{B}_{R_1})$	0.0038
$\delta(m_s)$	0.0024
$\delta(\Lambda_{QCD})$	0.0023
$\delta(B_{R_3})$	0.0023
$\delta(B_{R_1})$	0.0018
$\delta(\gamma)$	0.0001
$\delta(\lvert V_{ub}/V_{cb}\rvert)$	0
$\delta(\lvert V_{cb}\rvert)$	0
$\sum\delta$	0.125

Table D.8 Error breakdown for the ratio $\Delta\Gamma_d/\Delta M_d$

Parameter	Error contribution (%)
$\delta(\mu)$	0.0929
$\delta(B_3)$	0.0809
$\delta(B_{R_2})$	0.0623
$\delta(B_{R_0})$	0.0533
$\delta(\bar{z})$	0.0109
$\delta(m_b)$	0.0076
$\delta(m_t)$	0.0066
$\delta(\gamma)$	0.0025
$\delta(B_{R_3})$	0.0023
$\delta(\Lambda_{QCD})$	0.0022
$\delta(\lvert V_{ub}/V_{cb}\rvert)$	0.0009
$\delta(\tilde{B}_{R_1})$	0.0
$\delta(m_d)$	0.0
$\delta(B_{R_1})$	0.0
$\delta(\lvert V_{cb}\rvert)$	0.0
$\sum\delta$	0.149

Table D.9 Error breakdown for a_{sl}^{s}

Parameter	Error contribution (%)
$\delta(\mu)$	0.0946
$\delta(\bar{z})$	0.0463
$\delta(V_{ub}/V_{cb})$	0.0211
$\delta(\gamma)$	0.0118
$\delta(B_{R3})$	0.0106
$\delta(m_b)$	0.0101
$\delta(m_t)$	0.0066
$\delta(B_S)$	0.0078
$\delta(\Lambda_{QCD})$	0.0053
$\delta(B_{R2})$	0.0039
$\delta(\tilde{B}_{R1})$	0.0030
$\delta(B_{R0})$	0.0026
$\delta(m_s)$	0.0021
$\delta(B_{R1})$	0.0002
$\delta(V_{cb})$	0
$\sum \delta$	0.1098

Table D.10 Error breakdown for a_{sl}^{d}

Parameter	Error contribution (%)
$\delta(\mu)$	0.0937
$\delta(\bar{z})$	0.0487
$\delta(\lvert V_{ub}/V_{cb}\rvert)$	0.0215
$\delta(m_b)$	0.0129
$\delta(B_3)$	0.0123
$\delta(B_{R3})$	0.0115
$\delta(\gamma)$	0.0105
$\delta(m_t)$	0.0066
$\delta(\Lambda_{QCD})$	0.0054
$\delta(B_{R0})$	0.0049
$\delta(B_{R2})$	0.0042
$\delta(\tilde{B}_{R1})$	0.0
$\delta(m_d)$	0.0
$\delta(B_{R1})$	0.0
$\delta(\lvert V_{cb}\rvert)$	0.0
$\sum \delta$	0.111

D.2 Proof of $\Delta\Gamma \leq 2|\Gamma_{12}|$

In the B system we get the very simple expression Eq. 2.4.16 for the mixing observables ΔM and $\Delta\Gamma$ in terms of M_{12} and Γ_{12}, by expanding in the small parameter $\Delta\Gamma/\Delta M$. In the D system $\Delta\Gamma$ and ΔM are of the same order and so one would have to exactly solve the two defining equations. One can find however, the inequality $\Delta\Gamma \leq 2|\Gamma_{12}|$, which gives us the opportunity to calculate only Γ_{12} and to give an upper bound on $\Delta\Gamma$.

We start with the two fundamental equations for the mixing observables:

$$(\Delta M)^2 - \frac{1}{4}(\Delta\Gamma)^2 = 4|M_{12}|^2 - |\Gamma_{12}|^2\,, \tag{D.2.1}$$

$$\Delta M \Delta\Gamma = 4|M_{12}||\Gamma_{12}|\cos\phi_{12}\,. \tag{D.2.2}$$

Next we eliminate ΔM by substituting Eq. D.2.2 into Eq. D.2.1, and then solve for $|M_{12}|$.

$$\begin{aligned}
\frac{16|M_{12}|^2|\Gamma_{12}|^2\cos^2\phi_{12}}{(\Delta\Gamma)^2} - \frac{1}{4}(\Delta\Gamma)^2 &= 4|M_{12}|^2 - |\Gamma_{12}|^2 \\
|M_{12}|^2\left(\frac{16|\Gamma_{12}|^2\cos^2\phi_{12}}{(\Delta\Gamma)^2} - 4\right) &= \frac{1}{4}(\Delta\Gamma)^2 - |\Gamma_{12}|^2 \\
|M_{12}|^2 &= \frac{\frac{1}{4}(\Delta\Gamma)^2 - |\Gamma_{12}|^2}{\left(\frac{16|\Gamma_{12}|^2\cos^2\phi_{12}}{(\Delta\Gamma)^2} - 4\right)}\,.
\end{aligned} \tag{D.2.3}$$

Since $|M_{12}|^2 \geq 0$, we can say that the numerator and denominator on the right hand side of the last line of Eq. D.2.3 must have the same sign.

First, assume both terms are ≥ 0:

$$\frac{1}{4}(\Delta\Gamma)^2 - |\Gamma_{12}|^2 \geq 0 \quad \text{and} \quad \frac{16|\Gamma 12|^2\cos^2\phi_{12}}{(\Delta\Gamma)^2} - 4 \geq 0 \tag{D.2.4}$$

$$\Longrightarrow (\Delta\Gamma)^2 \geq 4|\Gamma_{12}|^2 \quad \text{and} \quad (\Delta\Gamma)^2 \leq 4\Gamma_{12}^2\cos^2\phi_{12}\,. \tag{D.2.5}$$

These inequalities are only consistent in the case $\cos^2\phi_{12} = 1$ and $\Delta\Gamma = 2|\Gamma_{12}|$.

Now, assume both terms are ≤ 0:

$$\frac{1}{4}(\Delta\Gamma)^2 - |\Gamma_{12}|^2 \leq 0 \quad \text{and} \quad \frac{16|\Gamma 12|^2\cos^2\phi_{12}}{(\Delta\Gamma)^2} - 4 \leq 0 \tag{D.2.6}$$

$$\Longrightarrow (\Delta\Gamma)^2 \leq 4|\Gamma_{12}|^2 \quad \text{and} \quad 4\Gamma_{12}^2\cos^2\phi_{12} \leq (\Delta\Gamma)^2\,. \tag{D.2.7}$$

As $0 \leq \cos^2 \phi_{12} \leq 1$, these inequalities are consistent for either a) $\cos^2 \phi_{12} = 1$ which gives $\Delta\Gamma = 2|\Gamma_{12}|$ or b) $2|\Gamma_{12}||\cos \phi_{12}| \leq \Delta\Gamma \leq 2|\Gamma_{12}|$.

We see that for either assumption the inequality $\Delta\Gamma \leq 2|\Gamma_{12}|$ holds. A similar line of reasoning shows that the inequality $\Delta M \leq 2|M_{12}|$ also holds.

Reference

1. Artuso M, Borissov G, Lenz A (2016) CP violation in the B_s^0 system. Rev Mod Phys 88:045002. https://doi.org/10.1103/RevModPhys.88.045002, arXiv:1511.09466

Appendix E
Additional Information from "Charming Dark Matter"

In this appendix we present more information on the work in Chap. 4.

In Appendix E.1 we explicitly give the Wilson coefficients that arise when considering contributions to rare D decays, in Appendix E.2 we give more information on our technique for calculating constraints from direct detection experiments, and in Appendix E.3 we show some of the Feynman diagrams that contribute to collider signatures for dark matter.

E.1 Rare Decays

The non-zero Wilson coefficients arise from electroweak penguins (shown in Fig. E.1) and (neglecting Z penguins since the small momentum transfer means they amount to an $\mathcal{O}(1)\%$ correction) we find

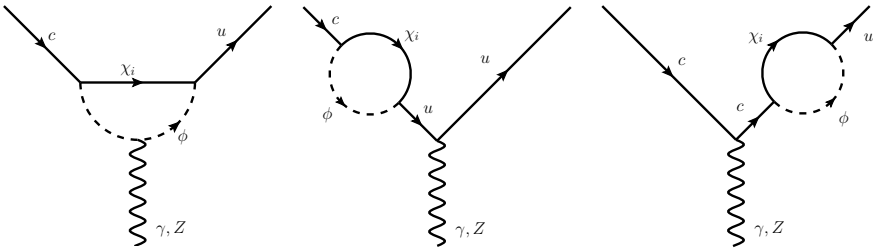

Fig. E.1 The DMFV model contribution to the effective operators governing rare decays of charm mesons, including explicit self-energy corrections to the external quark legs as explained in the text. The γ, Z couple to a lepton pair

M. J. Kirk, *Charming New Physics in Beautiful Processes?*,
Springer Theses, https://doi.org/10.1007/978-3-030-19197-9

$$C_7' = \sum_i \frac{\lambda_{1i}\lambda_{2i}^*}{6\sqrt{2}G_F}\Big[\; C_1(m_c^2, q^2, 0, m_{\chi_i}^2, m_\phi^2, m_\phi^2) + C_{11}(m_c^2, q^2, 0, m_{\chi_i}^2, m_\phi^2, m_\phi^2) + C_{12}(m_c^2, q^2, 0, m_{\chi_i}^2, m_\phi^2, m_\phi^2)\Big], \tag{E.1.1}$$

$$C_9' = \sum_i \frac{\lambda_{1i}\lambda_{2i}^*}{3\sqrt{2}G_F q^2}\Big[\; B_1(m_c^2, m_{\chi_i}^2, m_\phi^2) + 2C_{00}(m_c^2, q^2, 0, m_{\chi_i}^2, m_\phi^2, m_\phi^2) + m_c^2\Big\{\; C_1(m_c^2, q^2, 0, m_{\chi_i}^2, m_\phi^2, m_\phi^2) + C_{11}(m_c^2, q^2, 0, m_{\chi_i}^2, m_\phi^2, m_\phi^2) + C_{12}(m_c^2, q^2, 0, m_{\chi_i}^2, m_\phi^2, m_\phi^2)\Big\}\Big], \tag{E.1.2}$$

where B and C are loop functions using LoopTools [1] notation.

E.2 Direct Detection

E.2.1 LUX

For situations where we have both a measured event count N_k^{obs} (binned into energy bins labelled by k), and theoretical background N_k^{bck}, we can use the *likelihood ratio test*, a method based on a hypothesis test between a background only, and background+signal model, with likelihoods $\mathcal{L}$, $\mathcal{L}_{\text{bck}}$ respectively [2].

The likelihood of observing the data, D, assuming a particular set of parameters $\{\lambda\}$, is denoted $\mathcal{L}(D|\{\lambda\})$. The likelihood of each bin is a Poisson distribution $\text{Poiss}(N^{\text{obs}}, N^{\text{th}}(\lambda))$ where N_k^{th} are the predicted number of signal events (including background):

$$\mathcal{L}(N^{\text{obs}}|\{\lambda\}) = \prod_k \frac{\left(N_k^{\text{th}}\right)^{N_k^{\text{obs}}}}{N_k^{\text{obs}}!}\exp\left[-N_k^{\text{th}}\right] \tag{E.2.1}$$

and where $N^{\text{th}}(\lambda) = N^{\text{DM}}(\lambda) + N^{\text{bck}}$. The background only model is identical but with $N^{\text{th}} = N^{\text{bck}}$. Then the test statistic

$$\text{TS}(\lambda) = -2\log\left(\frac{\mathcal{L}}{\mathcal{L}_{\text{bck}}}\right) \approx 2\sum_k \left(N_k^{\text{th}} - N_k^{\text{obs}}\log\left[\frac{N_k^{\text{th}} + N_k^{\text{bck}}}{N_k^{\text{bck}}}\right]\right) \tag{E.2.2}$$

follows a χ^2 distribution—the cumulative probability density function of $\chi^2(x)$ represents the probability that we observe the data given the model parameters λ. The value of x such that $\chi^2(x) = C$ (i.e. the $C\%$ confidence limit) depends on the number of parameters $\{\lambda\}$—for only one parameter for example one can look up that $\chi^2(2.71) = 0.9$, which means that the 90% confidence bounds on λ are given by $\text{TS}(\lambda) = 2.71$.

E.2.2 CDMSlite

For CDMSlite, we use a conservative method based on the statement that the 90% confidence limit is such that *there is a probability of 0.9 that if the model were true, then the experiment would have measured more events (n) than have been measured ($n_{\rm obs}$)*. Using the Poisson distribution this probability is

$$P(n > n_{\rm obs}|\mu) = \sum_{n=n_{\rm obs}}^{\infty} \frac{\mu^n}{n!} \exp(-\mu) \approx \int_{n_{\rm obs}}^{\infty} \frac{1}{\sqrt{2\pi\mu}} \exp\left(-\frac{(t-\mu)^2}{2\mu}\right) dt = 0.9 \tag{E.2.3}$$

and in the limit $n_{\rm obs} \gg 1$, this can be approximated by

$$P(n > n_{\rm obs}|\mu) = \frac{1}{2}\left(\text{Erfc}\left(\frac{n_{\rm obs}-\mu}{\sqrt{2\mu}}\right)\right) = 0.9\,. \tag{E.2.4}$$

This equation is numerically solvable for μ giving a required signal $\mu = 109^{+51}_{-50}$, 88 ± 14, 635 ± 37 and 207 ± 20 events for energy bins 1–4 respectively. This is conservative since a large portion of the measured events are background, and the resulting limits are slightly weaker than those given by the CDMSlite collaboration.

E.3 Feynman Diagrams for Collider Searches

E.3.1 Monojet Processes

The dominant diagrams contributing to the pure monojet process are shown here. Each processes scales as $\sigma \propto (\lambda\lambda^{\dagger})\alpha_s$ and can become extremely large for large λ. The cross section is dominated by the diagrams containing a heavy ϕ resonance.

E.3.2 Dijet Processes

The dominant processes contributing to the production of on-shell ϕ, which decay $\phi \to q_i \chi_j$ producing a dijet signal, are shown in Figs. E.2 and E.3. In monojet analyses, this provides a subdominant contribution compared with pure monojet processes (Figs. E.4 and E.5) in most of the parameter space.

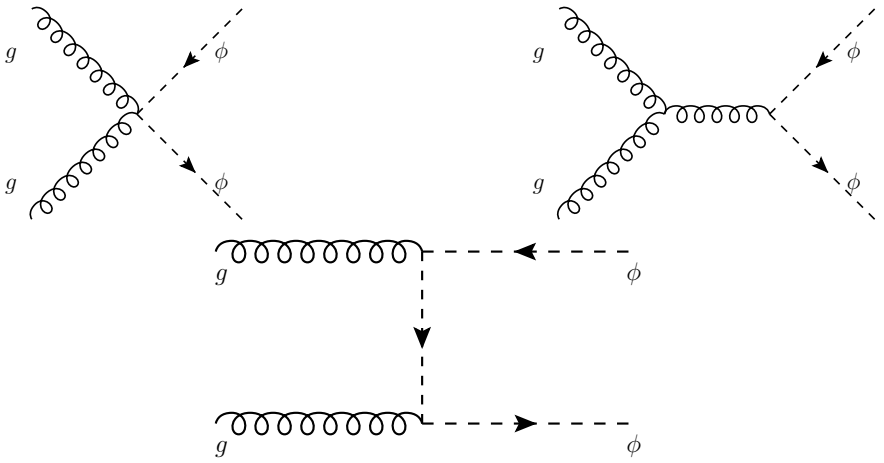

Fig. E.2 Gluon fusion dijet processes $\sigma \propto \alpha_s^2$

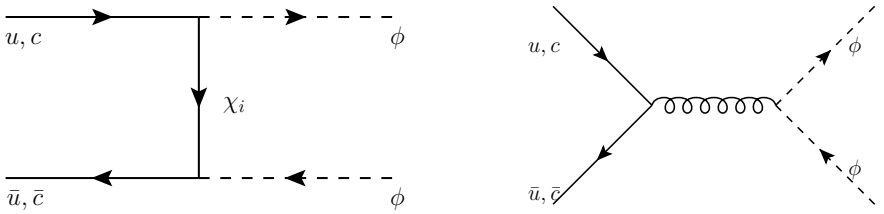

Fig. E.3 The left (right) process has $\sigma \propto (\lambda\lambda^\dagger)^2(\alpha_s^2)$ and so the dominance depends on the size of the new couplings—for couplings which are large enough to be excluded it is usually the left diagram which dominates

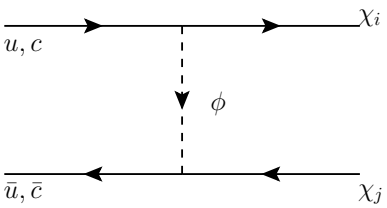

Fig. E.4 The above diagram must include initial/final state radiation from external legs or internal bremsstrahlung from the mediator. The contribution is roughly equal amongst these emissions

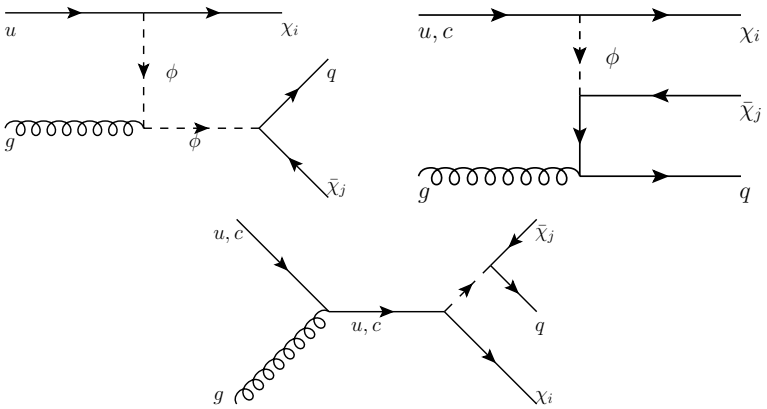

Fig. E.5 The s-channel ϕ resonance is responsible for top left and bottom dominating over top right, and the additional enhancement due to the gluon pdf over Fig. E.4 makes these the overall dominant monojet contribution. For very heavy mediators top left is suppressed due to the two propagators

References

1. Hahn T, Perez-Victoria M (1999) Automatized one loop calculations in four-dimensions and D-dimensions. Comput Phys Commun 118:153–165. https://doi.org/10.1016/S0010-4655(98)00173-8, arXiv:hep-ph/9807565
2. Cirelli M, Del Nobile E, Panci P (2013) Tools for model-independent bounds in direct dark matter searches. JCAP 1310:019. https://doi.org/10.1088/1475-7516/2013/10/019, arXiv:1307.5955

Appendix F
Additional Information from "Charming New Physics in Rare B_s Decays and Mixing?"

In this appendix we provide additional information on the technical aspects of our results for the anomalous dimensions entering in the RGE (Eq. 5.6.1) in Chap. 5.

A set of Wilson coefficients that contains C_7, C_9, and $C^c_{1\ldots4}$ and is closed under renormalisation necessarily also contains four QCD-penguin coefficients C_{P_i} multiplying the operators $P_{3\ldots6}$ (we define them as in [1]) and the chromodipole coefficient C_{8g}, resulting in an 11×11 anomalous dimension matrix γ. If the rescaled semileptonic operator $\tilde{Q}_9(\mu) = (4\pi/\alpha_s(\mu))Q_{9V}(\mu)$ is used, then to leading order $\gamma_{ij}(\mu) = \alpha_s(\mu)/(4\pi)\gamma^{(0)}_{ij}$, with constant $\gamma^{(0)}_{ij}$. As is well known, this matrix is already scheme-dependent at LO [2–4]. A scheme-independent matrix $\gamma^{\text{eff}(0)}$ can be achieved by replacing C_7 and C_8 by the scheme-independent combinations

$$C_7^{\text{eff}} = C_7 + \sum_i y_i C_i \,, \tag{F.0.1}$$

$$C_8^{\text{eff}} = C_8 + \sum_i z_i C_i \,, \tag{F.0.2}$$

where

$$\langle s\gamma|Q_i|b\rangle = y_i \langle s\gamma|Q_{7\gamma}|b\rangle \,, \tag{F.0.3}$$

$$\langle sg|Q_i|b\rangle = z_i \langle s\gamma|Q_{8g}|b\rangle \,, \tag{F.0.4}$$

to lowest order and the sums run over all four-quark operators. We find that y_i and z_i vanish for $Q^c_{1\ldots4}$, leaving only the known coefficients $y_{P_i} = (-1/3, -4/9, -20/3, -80/9)_i$ and $z_{P_i} = (1, -1/6, 20, -10/3)_i$ $(i = 3\ldots6)$ [1]. The BSM correction ΔC_9^{eff} in Eqs. 5.3.2 and 5.3.7 coincides with the (BSM correction to the) coefficient C_9 of Q_{9V} to LL accuracy.

Many of the elements of $\gamma^{\text{eff}(0)}$ are known [2, 3, 5–11], except for $\gamma^{\text{eff}(0)}_{Q_i^c Q_{7\gamma}}$, $\gamma^{\text{eff}(0)}_{Q_i^c Q_{8g}}$, $\gamma^{\text{eff}(0)}_{Q_i^c P_j}$, and $\gamma^{\text{eff}(0)}_{Q_i^c \tilde{Q}_9}$, for $i = 3, 4$. The latter can be read off from the logarithmic terms in Eq. 5.3.2, and the mixing into P_i follows from substituting gauge coupling and

M. J. Kirk, *Charming New Physics in Beautiful Processes?*,
Springer Theses, https://doi.org/10.1007/978-3-030-19197-9

colour factors in the diagram shown on the left of Fig. 5.1. This gives

$$\gamma^{(0)}_{Q_i^c \tilde{Q}_9} = \left(-\frac{8}{3}, -\frac{8}{9}, \frac{4}{3}, \frac{4}{9}\right)_i , \quad \gamma^{(0)}_{Q_i^c P_4} = \left(0, \frac{4}{3}, 0, -\frac{2}{3}\right)_i ,$$

for $i = 1, 2, 3, 4$, with the mixing into $C_{P_{3,5,6}}$ vanishing.

The leading mixing into C_7^{eff} arises at two loops [12–15] and is the technically most challenging aspect of our results. Our calculation employs the 1PI (off-shell) formalism and the method of [16] for computing UV divergences, which involves an infrared-regulator mass and the appearance of a set of gauge-non-invariant counterterms. The result is

$$\gamma^{\text{eff}(0)}_{Q_i^c Q_7} = \left(0, \frac{416}{81}, 0, \frac{224}{81}\right)_i \qquad (i = 1, 2, 3, 4) .$$

Our stated results for $i = 1, 2$ agree with the results in [1, 9], which constitutes a cross-check of our calculation.

We have not obtained the 2-loop mixing of $C^c_{3,4}$ into C_{8g} and set these anomalous dimension elements to zero. For the case of $C^c_{1,2}$ where this mixing is known, the impact of neglecting $\gamma^{\text{eff}(0)}_{i8}$ on $\Delta C_7^{\text{eff}}(\mu)$ is small (the only change being $-0.19\Delta C_2 \to -0.18\Delta C_2$ in Eq. 5.3.6). We expect a similarly small error in the case of $\Delta C_{3,4}$.

References

1. Chetyrkin KG, Misiak M, Munz M (1997) Weak radiative B meson decay beyond leading logarithms. Phys Lett B 400:206–219. https://doi.org/10.1016/S0370-2693(97)00324-9, arXiv:hep-ph/9612313
2. Ciuchini M, Franco E, Martinelli G, Reina L, Silvestrini L (1993) Scheme independence of the effective Hamiltonian for $b \to s\gamma$ and $b \to sg$ decays. Phys Lett B 316:127–136. https://doi.org/10.1016/0370-2693(93)90668-8, arXiv:hep-ph/9307364
3. Ciuchini M, Franco E, Martinelli G, Reina L, Silvestrini L (1994) $b \to s\gamma$ and $b \to sg$: a theoretical reappraisal. Phys Lett B 334:137–144. https://doi.org/10.1016/0370-2693(94)90602-5, arXiv:hep-ph/9406239
4. Ciuchini M, Franco E, Reina L, Silvestrini L (1994) Leading order QCD corrections to $b \to s\gamma$ and $b \to sg$ decays in three regularization schemes. Nucl Phys B 421:41–64. https://doi.org/10.1016/0550-3213(94)90223-2, arXiv:hep-ph/9311357
5. Gaillard MK, Lee BW (1974) Δ I = 1/2 Rule for nonleptonic decays in asymptotically free field theories. Phys Rev Lett 33:108. https://doi.org/10.1103/PhysRevLett.33.108
6. Altarelli G, Maiani L (1974) Octet enhancement of nonleptonic weak interactions in asymptotically free gauge theories. Phys Lett B 52:351–354. https://doi.org/10.1016/0370-2693(74)90060-4
7. Gilman FJ, Wise MB (1979) Effective Hamiltonian for $\Delta S = 1$ weak nonleptonic decays in the six quark model. Phys Rev D 20:2392. https://doi.org/10.1103/PhysRevD.20.2392
8. Shifman MA, Vainshtein AI, Zakharov VI (1977) Nonleptonic decays of K mesons and hyperons. Sov Phys JETP 45:670
9. Gilman FJ, Wise MB (1980) $K \to \pi e^+ e^-$ in the Six Quark Model. Phys Rev D 21:3150. https://doi.org/10.1103/PhysRevD.21.3150

10. Guberina B, Peccei RD (1980) Quantum Chromodynamic Effects and CP Violation in the Kobayashi-Maskawa Model. Nucl Phys B 163:289–311. https://doi.org/10.1016/0550-3213(80)90404-6
11. Buras AJ, Misiak M, Urban J (2000) Two loop QCD anomalous dimensions of flavor changing four quark operators within and beyond the standard model. Nucl Phys B 586:397–426. https://doi.org/10.1016/S0550-3213(00)00437-5, arXiv:hep-ph/0005183
12. Bertolini S, Borzumati F, Masiero A (1987) QCD enhancement of radiative B decays. Phys Rev Lett 59:180. https://doi.org/10.1103/PhysRevLett.59.180
13. Grinstein B, Springer RP, Wise MB (1988) Effective Hamiltonian for weak radiative B meson decay. Phys Lett B 202:138–144. https://doi.org/10.1016/0370-2693(88)90868-4
14. Grinstein B, Springer RP, Wise MB (1990) Strong interaction effects in weak radiative $\bar{B}$ meson decay. Nucl Phys B 339:269–309. https://doi.org/10.1016/0550-3213(90)90350-M
15. Misiak M (1991) QCD corrected effective Hamiltonian for the $b \to s\gamma$ decay. Phys Lett B 269:161–168. https://doi.org/10.1016/0370-2693(91)91469-C
16. Chetyrkin KG, Misiak M, Munz M (1998) Beta functions and anomalous dimensions up to three loops. Nucl Phys B 518:473–494. https://doi.org/10.1016/S0550-3213(98)00122-9, arXiv:hep-ph/9711266

Appendix G
Additional Information from "Dimension-Six Matrix Elements from Sum Rules"

In this appendix we provide additional information relating to our work in Chap. 6.

In Appendix G.1 we provide our choice of basis for the evanescent operators for both the $\Delta B = 2$ and $\Delta B = 0$ sectors, along with the corresponding anomalous dimension matrices.

In Appendix G.2 we show our choice of input parameters (Table G.1) as well as a detailed breakdown of the uncertainties associated with our results for the bag parameters (Tables G.2, G.3, G.4 and G.5).

Finally in Tables G.6, G.7 G.8 and G.9 we provide a breakdown of the errors in our mixing and lifetime ratio observables.

G.1 Basis of Evanescent Operators and ADMs

G.1.1 $\Delta B = 2$ *Operators*

Our choice of basis for the evanescent operators is given by

$$
\begin{aligned}
E_1 &= \bar{b}_i\gamma_\mu(1-\gamma^5)q_j\ \bar{b}_j\gamma^\mu(1-\gamma^5)q_i - Q_1\,,\\
E_2 &= \bar{b}_i\gamma_\mu\gamma_\nu(1-\gamma^5)q_i\ \bar{b}_j\gamma^\mu\gamma^\nu(1-\gamma^5)q_j - (8-4\epsilon)Q_2 - (8-8\epsilon)Q_3\,,\\
E_3 &= \bar{b}_i\gamma_\mu\gamma_\nu(1-\gamma^5)q_j\ \bar{b}_j\gamma^\mu\gamma^\nu(1-\gamma^5)q_i - (8-8\epsilon)Q_2 - (8-4\epsilon)Q_3\,,\\
E_4 &= \bar{b}_i\gamma_\mu\gamma_\nu\gamma_\rho(1-\gamma^5)q_i\ \bar{b}_j\gamma^\mu\gamma^\nu\gamma^\rho(1-\gamma^5)q_j - (16-4\epsilon)Q_1\,,\\
E_5 &= \bar{b}_i\gamma_\mu\gamma_\nu\gamma_\rho(1-\gamma^5)q_j\ \bar{b}_j\gamma^\mu\gamma^\nu\gamma^\rho(1-\gamma^5)q_i - (16-4\epsilon)(Q_1+E_1)\,,\\
E_6 &= \bar{b}_i\gamma_\mu(1-\gamma^5)q_i\ \bar{b}_j\gamma^\mu(1+\gamma^5)q_j + 2Q_5\,,\\
E_7 &= \bar{b}_i\gamma_\mu(1-\gamma^5)q_j\ \bar{b}_j\gamma^\mu(1+\gamma^5)q_i + 2Q_4\,,\\
E_8 &= \bar{b}_i\gamma_\mu\gamma_\nu(1-\gamma^5)q_i\ \bar{b}_j\gamma^\mu\gamma^\nu(1+\gamma^5)q_j - 4Q_4\,,\\
E_9 &= \bar{b}_i\gamma_\mu\gamma_\nu(1-\gamma^5)q_j\ \bar{b}_j\gamma^\mu\gamma^\nu(1+\gamma^5)q_i - 4Q_5\,,
\end{aligned}
\tag{G.1.1}
$$

M. J. Kirk, *Charming New Physics in Beautiful Processes?*,
Springer Theses, https://doi.org/10.1007/978-3-030-19197-9

for QCD and

$$
\begin{aligned}
\tilde{E}_1 &= \bar{h}_i^{\{(+)} \gamma_\mu (1-\gamma^5) q_j \; \bar{h}_j^{(-)\}} \gamma^\mu (1-\gamma^5) q_i - \tilde{Q}_1 \,, \\
\tilde{E}_2 &= \frac{1}{2}\tilde{Q}_1 + \tilde{Q}_2 + \bar{h}_i^{\{(+)} (1-\gamma^5) q_j \; \bar{h}_j^{(-)\}} (1-\gamma^5) q_i \,, \\
\tilde{E}_3 &= \bar{h}_i^{\{(+)} \gamma_\mu \gamma_\nu (1-\gamma^5) q_i \; \bar{h}_j^{(-)\}} \gamma^\mu \gamma^\nu (1-\gamma^5) q_j + (4+a_1\epsilon)\tilde{Q}_1 \,, \\
\tilde{E}_4 &= \bar{h}_i^{\{(+)} \gamma_\mu \gamma_\nu (1-\gamma^5) q_j \; \bar{h}_j^{(-)\}} \gamma^\mu \gamma^\nu (1-\gamma^5) q_i + (4+a_1\epsilon)(\tilde{Q}_1 + \tilde{E}_1) \,, \\
\tilde{E}_5 &= \bar{h}_i^{\{(+)} \gamma_\mu \gamma_\nu \gamma_\rho (1-\gamma^5) q_i \; \bar{h}_j^{(-)\}} \gamma^\mu \gamma^\nu \gamma^\rho (1-\gamma^5) q_j - (16+a_2\epsilon)\tilde{Q}_1 \,, \\
\tilde{E}_6 &= \bar{h}_i^{\{(+)} \gamma_\mu \gamma_\nu \gamma_\rho (1-\gamma^5) q_j \; \bar{h}_j^{(-)\}} \gamma^\mu \gamma^\nu \gamma^\rho (1-\gamma^5) q_i - (16+a_2\epsilon)(\tilde{Q}_1 + \tilde{E}_1) \,, \\
\tilde{E}_7 &= \bar{h}_i^{\{(+)} \gamma_\mu (1-\gamma^5) q_i \; \bar{h}_j^{(-)\}} \gamma^\mu (1+\gamma^5) q_j + 2\tilde{Q}_5 \,, \\
\tilde{E}_8 &= \bar{h}_i^{\{(+)} \gamma_\mu (1-\gamma^5) q_j \; \bar{h}_j^{(-)\}} \gamma^\mu (1+\gamma^5) q_i + 2\tilde{Q}_4 \,, \\
\tilde{E}_9 &= \bar{h}_i^{\{(+)} \gamma_\mu \gamma_\nu (1-\gamma^5) q_i \; \bar{h}_j^{(-)\}} \gamma^\mu \gamma^\nu (1+\gamma^5) q_j - (4+a_3\epsilon)\tilde{Q}_4 \,, \\
\tilde{E}_{10} &= \bar{h}_i^{\{(+)} \gamma_\mu \gamma_\nu (1-\gamma^5) q_j \; \bar{h}_j^{(-)\}} \gamma^\mu \gamma^\nu (1+\gamma^5) q_i - (4+a_3\epsilon)\tilde{Q}_5 \,,
\end{aligned}
\tag{G.1.2}
$$

for HQET. It is straightforward to verify that the evanescent operators vanish in four dimensions by using the Fierz identities Eqs. A.0.2, A.0.4 and A.0.5 along with the relation

$$
\gamma_\mu \gamma_\nu \gamma_\rho = g_{\mu\nu}\gamma_\rho + g_{\nu\rho}\gamma_\mu - g_{\mu\rho}\gamma_\nu - i\epsilon_{\mu\nu\rho\lambda}\gamma^\lambda \gamma^5 . \tag{G.1.3}
$$

A useful strategy to simplify expressions with two Dirac matrices is to use projection identities, e.g.

$$
\bar{h}^{(\pm)} \gamma_\mu \gamma_\nu (1-\gamma^5) q = \pm \bar{h}^{(\pm)} \not{v} \gamma_\mu \gamma_\nu (1-\gamma^5) q, \tag{G.1.4}
$$

and then reduce the number of Dirac matrices with Eq. G.1.3.

In the decomposition shown in Eq. 6.2.8 the LO QCD ADM is

$$
\gamma_{QQ}^{(0)} = \begin{pmatrix}
\frac{6(N_c-1)}{N_c} & 0 & 0 & 0 & 0 \\
0 & -\frac{2\left(3N_c^2-4N_c-1\right)}{N_c} & \frac{4N_c-8}{N_c} & 0 & 0 \\
0 & \frac{4(N_c-2)(N_c+1)}{N_c} & \frac{2(N_c+1)^2}{N_c} & 0 & 0 \\
0 & 0 & 0 & -\frac{6(N_c^2-1)}{N_c} & 0 \\
0 & 0 & 0 & -6 & \frac{6}{N_c}
\end{pmatrix} , \tag{G.1.5}
$$

$$\gamma^{(0)}_{QE} = \begin{pmatrix} 6 & 0 & 0 & -\frac{1}{N_c} & 1 & 0 & 0 & 0 & 0 \\ 0 & -\frac{1}{N_c} & 1 & 0 & 0 & 0 & 0 & 0 & 0 \\ 0 & \frac{1}{2} & \frac{N_c}{2} - \frac{1}{N_c} & 0 & 0 & 0 & 0 & 0 & 0 \\ 0 & 0 & 0 & 0 & 0 & 0 & 0 & -\frac{1}{N_c} & 1 \\ 0 & 0 & 0 & 0 & 0 & 0 & 0 & \frac{1}{2} & \frac{N_c}{2} - \frac{1}{N_c} \end{pmatrix} . \tag{G.1.6}$$

In HQET we find

$$\tilde{\gamma}^{(0)}_{\tilde{Q}\tilde{Q}} = \begin{pmatrix} \frac{3}{N_c} - 3N_c & 0 & 0 & 0 \\ 1 + \frac{1}{N_c} & -3N_c + 4 + \frac{7}{N_c} & 0 & 0 \\ 0 & 0 & \frac{6}{N_c} - 3N_c & -3 \\ 0 & 0 & -3 & \frac{6}{N_c} - 3N_c \end{pmatrix} , \tag{G.1.7}$$

$$\tilde{\gamma}^{(0)}_{\tilde{Q}\tilde{E}} = \begin{pmatrix} 0 & 0 & 0 & 0 & -\frac{1}{4N_c} & \frac{1}{4} & 0 & 0 & 0 & 0 \\ -1 & -4 & -\frac{1}{4N_c} & \frac{1}{4} & 0 & 0 & 0 & 0 & 0 & 0 \\ 0 & 0 & 0 & 0 & 0 & 0 & 0 & -\frac{1}{4N_c} & \frac{1}{4} \\ 0 & 0 & 0 & 0 & 0 & 0 & 0 & \frac{1}{4} & -\frac{1}{4N_c} \end{pmatrix} . \tag{G.1.8}$$

Our result (Eq. G.1.5) with $N_c = 3$ differs from the results of [1, 2] because we have only used the replacements implied by the basis of evanescent operators (Eq. G.1.1) to simplify products of Dirac matrices. We can reproduce their result by applying 4-dimensional Fierz identities that relate Q_1, Q_2 and Q_3. The upper left 2×2 sub-matrix of Eq. G.1.7 agrees with [3].

G.1.2 $\Delta B = 0$ *Operators*

We define the basis of evanescent operators in QCD following [4]:

$$\begin{aligned} E^q_1 &= \bar{b}\gamma_\mu\gamma_\nu\gamma_\rho(1-\gamma^5)q\ \bar{q}\gamma^\rho\gamma^\nu\gamma^\mu(1-\gamma^5)b - (4-8\epsilon)Q^q_1 , \\ E^q_2 &= \bar{b}\gamma_\mu\gamma_\nu(1-\gamma^5)q\ \bar{q}\gamma^\nu\gamma^\mu(1+\gamma^5)b - (4-8\epsilon)Q^q_2 , \\ E^q_3 &= \bar{b}\gamma_\mu\gamma_\nu\gamma_\rho(1-\gamma^5)T^A q\ \bar{q}\gamma^\rho\gamma^\nu\gamma^\mu(1-\gamma^5)T^A b - (4-8\epsilon)T^q_1 , \\ E^q_4 &= \bar{b}\gamma_\mu\gamma_\nu(1-\gamma^5)T^A q\ \bar{q}\gamma^\nu\gamma^\mu(1+\gamma^5)T^A b - (4-8\epsilon)T^q_2 . \end{aligned} \tag{G.1.9}$$

In HQET we again introduce parameters $a_{1,2}$ to keep track of the scheme dependence.

$$\begin{aligned}
\tilde{E}_1^q &= \bar{h}\gamma_\mu\gamma_\nu\gamma_\rho(1-\gamma^5)q\ \bar{q}\gamma^\rho\gamma^\nu\gamma^\mu(1-\gamma^5)h - (4+a_1\epsilon)\tilde{Q}_1^q\,,\\
\tilde{E}_2^q &= \bar{h}\gamma_\mu\gamma_\nu(1-\gamma^5)q\ \bar{q}\gamma^\nu\gamma^\mu(1+\gamma^5)h - (4+a_2\epsilon)\tilde{Q}_2^q\,,\\
\tilde{E}_3^q &= \bar{h}\gamma_\mu\gamma_\nu\gamma_\rho(1-\gamma^5)T^A q\ \bar{q}\gamma^\rho\gamma^\nu\gamma^\mu(1-\gamma^5)T^A h - (4+a_1\epsilon)\tilde{T}_1^q\,,\\
\tilde{E}_4^q &= \bar{h}\gamma_\mu\gamma_\nu(1-\gamma^5)T^A q\ \bar{q}\gamma^\nu\gamma^\mu(1+\gamma^5)T^A h - (4+a_2\epsilon)\tilde{T}_2^q\,.
\end{aligned} \tag{G.1.10}$$

The isospin breaking combinations of the evanescent operators are defined in analogy to Eq. 6.5.3. The LO ADM in QCD takes the form

$$\gamma_{QQ}^{(0)} = \begin{pmatrix} 0 & 0 & 12 & 0 \\ 0 & \frac{6}{N_c} - 6N_c & 0 & 0 \\ 3 - \frac{3}{N_c^2} & 0 & -\frac{12}{N_c} & 0 \\ 0 & 0 & 0 & \frac{6}{N_c} \end{pmatrix}, \tag{G.1.11}$$

$$\gamma_{QE}^{(0)} = \begin{pmatrix} 0 & 0 & -2 & 0 \\ 0 & 0 & 0 & -2 \\ \frac{1}{2N_c^2} - \frac{1}{2} & 0 & \frac{2}{N_c} - \frac{N_c}{2} & 0 \\ 0 & \frac{1}{2N_c^2} - \frac{1}{2} & 0 & \frac{2}{N_c} - \frac{N_c}{2} \end{pmatrix}. \tag{G.1.12}$$

The HQET result is given by

$$\tilde{\gamma}_{\tilde{Q}\tilde{Q}}^{(0)} = \begin{pmatrix} \frac{3}{N_c} - 3N_c & 0 & 6 & 0 \\ 0 & \frac{3}{N_c} - 3N_c & 0 & 6 \\ \frac{3}{2} - \frac{3}{2N_c^2} & 0 & -\frac{3}{N_c} & 0 \\ 0 & \frac{3}{2} - \frac{3}{2N_c^2} & 0 & -\frac{3}{N_c} \end{pmatrix}, \tag{G.1.13}$$

$$\tilde{\gamma}_{\tilde{Q}\tilde{E}}^{(0)} = \begin{pmatrix} 0 & 0 & -\frac{1}{2} & 0 \\ 0 & 0 & 0 & -\frac{1}{2} \\ \frac{1}{8N_c^2} - \frac{1}{8} & 0 & \frac{1}{2N_c} - \frac{N_c}{4} & 0 \\ 0 & \frac{1}{8N_c^2} - \frac{1}{8} & 0 & \frac{1}{2N_c} - \frac{N_c}{4} \end{pmatrix}. \tag{G.1.14}$$

Our result in Eq. G.1.11 is in agreement with [5, 6] and Eq. G.1.13 reproduces the result of [7].[2] The results in Eqs. G.1.12 and G.1.14 are new. The matching coefficients read

$$C_{Q_i\tilde{Q}_j}^{(0)} = \delta_{ij} \tag{G.1.15}$$

[2]Note that [7] contains a misprint that has been identified in [8].

at LO and

$$C^{(1)}_{Q_i\tilde{Q}_j} = \begin{pmatrix} -4L_\mu - \frac{32}{3} & \frac{16}{3} & -\frac{a_1}{4} - 3L_\mu - 13 & -2 \\ 0 & 4L_\mu + \frac{16}{3} & -\frac{3}{2} & -\frac{a_2}{4} + 3L_\mu - 1 \\ -\frac{a_1}{18} - \frac{2L_\mu}{3} - \frac{26}{9} & -\frac{4}{9} & -\frac{7a_1}{24} + \frac{3L_\mu}{2} + \frac{7}{6} & -3 \\ -\frac{1}{3} & -\frac{a_2}{18} + \frac{2L_\mu}{3} - \frac{2}{9} & -\frac{1}{4} & -\frac{7a_2}{24} - \frac{3L_\mu}{2} - \frac{29}{6} \end{pmatrix} \tag{G.1.16}$$

at NLO where we have set $N_c = 3$ for brevity.

G.2 Inputs and Detailed Overview of Uncertainties

Table G.1 Input values for parameters. Note that for f_B we use the mean of f_B and f_{B^+}, while for f_D we use the "experimental" value instead of the lattice average, since the former is in significantly better agreement with sum rule results [14–17]

Parameter	Value	Source
$\overline{m}_b(\overline{m}_b)$	$\left(4.203^{+0.016}_{-0.034}\right)$ GeV	[9, 10]
$m_b^{\rm PS}(2\,{\rm GeV})$	$\left(4.532^{+0.013}_{-0.039}\right)$ GeV	[9, 10]
$m_b^{\rm 1S}$	$\left(4.66^{+0.04}_{-0.03}\right)$ GeV	[11]
$m_b^{\rm kin}(1\,{\rm GeV})$	(4.553 ± 0.020) GeV	[12]
$\overline{m}_c(\overline{m}_c)$	(1.279 ± 0.013) GeV	[13]
$\alpha_s(M_Z)$	0.1181 ± 0.0011	[11]
V_{us}	0.2248 ± 0.0006	[11]
V_{ub}	0.00409 ± 0.00039	[11]
V_{cb}	0.0405 ± 0.0015	[11]
$\gamma_{\rm CKM}$	$\left(73.2^{+6.3}_{-7.0}\right)^\circ$	[11]
f_B	(189 ± 4) MeV	[11]
f_{B_s}	(227.2 ± 3.4) MeV	[11]
f_D	(203.7 ± 4.8) MeV	[11]

Table G.2 Individual errors for the bag parameters of the $\Delta B = 2$ matrix elements

	$\overline{\Lambda}$	Intrinsic SR	Condensates	μ_ρ	$1/m_b$	μ_m	a_i
$\overline{B}_{Q_1}$	$^{+0.001}_{-0.002}$	± 0.018	± 0.004	$^{+0.011}_{-0.022}$	± 0.010	$^{+0.045}_{-0.039}$	$^{+0.007}_{-0.007}$
$\overline{B}_{Q_2}$	$^{+0.014}_{-0.017}$	± 0.020	± 0.004	$^{+0.012}_{-0.019}$	± 0.010	$^{+0.071}_{-0.062}$	$^{+0.015}_{-0.015}$
$\overline{B}_{Q_3}$	$^{+0.060}_{-0.074}$	± 0.107	± 0.023	$^{+0.016}_{-0.008}$	± 0.010	$^{+0.086}_{-0.069}$	$^{+0.053}_{-0.052}$
$\overline{B}_{Q_4}$	$^{+0.007}_{-0.006}$	± 0.021	± 0.011	$^{+0.003}_{-0.003}$	± 0.010	$^{+0.088}_{-0.079}$	$^{+0.005}_{-0.006}$
$\overline{B}_{Q_5}$	$^{+0.019}_{-0.015}$	± 0.018	± 0.009	$^{+0.004}_{-0.006}$	± 0.010	$^{+0.077}_{-0.068}$	$^{+0.012}_{-0.012}$

Table G.3 Individual errors for the bag parameters of the $\Delta B = 0$ matrix elements

	$\overline{\Lambda}$	Intrinsic SR	Condensates	μ_ρ	$1/m_b$	μ_m	a_i
$\overline{B}_1$	$^{+0.003}_{-0.002}$	± 0.019	± 0.002	$^{+0.002}_{-0.002}$	± 0.010	$^{+0.060}_{-0.052}$	$^{+0.002}_{-0.003}$
$\overline{B}_2$	$^{+0.001}_{-0.001}$	± 0.020	± 0.002	$^{+0.000}_{-0.001}$	± 0.010	$^{+0.084}_{-0.076}$	$^{+0.001}_{-0.002}$
$\overline{\epsilon}_1$	$^{+0.006}_{-0.007}$	± 0.022	± 0.003	$^{+0.003}_{-0.003}$	± 0.010	$^{+0.010}_{-0.012}$	$^{+0.006}_{-0.007}$
$\overline{\epsilon}_2$	$^{+0.005}_{-0.006}$	± 0.017	± 0.003	$^{+0.002}_{-0.001}$	± 0.010	$^{+0.001}_{-0.002}$	$^{+0.003}_{-0.004}$

Table G.4 Individual errors for the bag parameters of the $\Delta C = 2$ matrix elements

	$\overline{\Lambda}$	Intrinsic SR	Condensates	μ_ρ	$1/m_c$	μ_m	a_i
$\overline{B}_{Q_1}$	$^{+0.001}_{-0.002}$	± 0.013	± 0.003	$^{+0.009}_{-0.021}$	± 0.030	$^{+0.039}_{-0.021}$	± 0.003
$\overline{B}_{Q_2}$	$^{+0.011}_{-0.014}$	± 0.015	± 0.003	$^{+0.010}_{-0.016}$	± 0.030	$^{+0.092}_{-0.050}$	± 0.012
$\overline{B}_{Q_3}$	$^{+0.037}_{-0.045}$	± 0.059	± 0.013	$^{+0.016}_{-0.016}$	± 0.030	$^{+0.116}_{-0.059}$	± 0.016
$\overline{B}_{Q_4}$	$^{+0.006}_{-0.005}$	± 0.017	± 0.009	$^{+0.003}_{-0.003}$	± 0.030	$^{+0.131}_{-0.071}$	± 0.004
$\overline{B}_{Q_5}$	$^{+0.014}_{-0.012}$	± 0.014	± 0.007	$^{+0.004}_{-0.005}$	± 0.030	$^{+0.127}_{-0.069}$	± 0.004

Table G.5 Individual errors for the bag parameters of the $\Delta C = 0$ matrix elements

	$\overline{\Lambda}$	Intrinsic SR	Condensates	μ_ρ	$1/m_c$	μ_m	a_i
$\overline{B}_1$	$^{+0.004}_{-0.003}$	± 0.017	± 0.002	$^{+0.002}_{-0.002}$	± 0.030	$^{+0.068}_{-0.037}$	$^{+0.003}_{-0.005}$
$\overline{B}_2$	$^{+0.001}_{-0.000}$	± 0.015	± 0.001	$^{+0.000}_{-0.000}$	± 0.030	$^{+0.120}_{-0.065}$	$^{+0.000}_{-0.001}$
$\overline{\epsilon}_1$	$^{+0.007}_{-0.008}$	± 0.024	± 0.004	$^{+0.003}_{-0.004}$	± 0.030	$^{+0.012}_{-0.022}$	$^{+0.006}_{-0.008}$
$\overline{\epsilon}_2$	$^{+0.003}_{-0.004}$	± 0.011	± 0.002	$^{+0.001}_{-0.001}$	± 0.030	$^{+0.000}_{-0.000}$	$^{+0.001}_{-0.002}$

Table G.6 Individual errors for the B_s mixing observables

Parameter	Error contribution		
	$\Delta M_s^{\rm SM}/{\rm ps}^{-1}$	$\Delta\Gamma_s^{\rm PS}/{\rm ps}^{-1}$	$a_{\rm sl}^{s,{\rm PS}}/10^{-5}$
$\delta(\overline{B}_{Q_1})$	± 1.1	± 0.005	± 0.01
$\delta(\overline{B}_{Q_3})$	± 0.0	± 0.005	± 0.01
$\delta(\overline{B}_{R_0})$	± 0.0	± 0.003	± 0.00
$\delta(\overline{B}_{R_1})$	± 0.0	± 0.000	± 0.00
$\delta(\overline{B}_{R_1'})$	± 0.0	± 0.000	± 0.00
$\delta(\overline{B}_{R_2})$	± 0.0	± 0.016	± 0.00
$\delta(\overline{B}_{R_3})$	± 0.0	± 0.001	± 0.02
$\delta(\overline{B}_{R_3'})$	± 0.0	± 0.000	± 0.05
$\delta(f_{B_s})$	± 0.5	± 0.002	± 0.00
$\delta(\mu_1)$	± 0.0	$^{+0.007}_{-0.018}$	$^{+0.04}_{-0.08}$
$\delta(\mu_2)$	± 0.1	$^{+0.000}_{-0.002}$	± 0.01
$\delta(m_b)$	± 0.0	$^{+0.000}_{-0.001}$	± 0.01
$\delta(m_c)$	± 0.0	$^{+0.000}_{-0.001}$	± 0.06
$\delta(\alpha_s)$	± 0.0	± 0.000	± 0.04
δ(CKM)	$^{+1.4}_{-1.3}$	± 0.006	$^{+0.21}_{-0.22}$

Table G.7 Individual errors for the B_d mixing observables

Parameter	Error contribution		
	$\Delta M_d^{\rm SM}/{\rm ps}^{-1}$	$\Delta\Gamma_d^{\rm PS}/10^{-3}\,{\rm ps}^{-1}$	$a_{\rm sl}^{d,\rm PS}/10^{-4}$
$\delta(\overline{B}_{Q_1})$	$^{+0.04}_{-0.03}$	±0.16	±0.02
$\delta(\overline{B}_{Q_3})$	±0.00	$^{+0.17}_{-0.16}$	±0.03
$\delta(\overline{B}_{R_0})$	±0.00	±0.11	±0.01
$\delta(\overline{B}_{R_1})$	±0.00	±0.01	±0.00
$\delta(\overline{B}_{R_1'})$	±0.00	±0.01	±0.00
$\delta(\overline{B}_{R_2})$	±0.00	±0.54	±0.00
$\delta(\overline{B}_{R_3})$	±0.00	±0.00	±0.04
$\delta(\overline{B}_{R_3'})$	±0.00	±0.01	±0.09
$\delta(f_B)$	±0.03	±0.11	±0.00
$\delta(\mu_1)$	±0.00	$^{+0.24}_{-0.62}$	$^{+0.17}_{-0.07}$
$\delta(\mu_2)$	±0.00	$^{+0.00}_{-0.08}$	$^{+0.01}_{-0.03}$
$\delta(m_b)$	±0.00	$^{+0.01}_{-0.03}$	$^{+0.01}_{-0.03}$
$\delta(m_c)$	±0.00	$^{+0.01}_{-0.02}$	±0.13
$\delta(\alpha_s)$	±0.00	±0.01	±0.08
δ(CKM)	±0.08	$^{+0.38}_{-0.37}$	$^{+0.47}_{-0.44}$

Table G.8 Individual errors for the ratio $\tau(B^+)/\tau(B^0)$ in the PS mass scheme

Parameter	Error contribution
$\delta(\overline{B}_1)$	±0.002
$\delta(\overline{B}_2)$	±0.000
$\delta(\overline{\epsilon}_1)$	$^{+0.016}_{-0.015}$
$\delta(\overline{\epsilon}_2)$	±0.004
$\delta(\rho_3)$	±0.001
$\delta(\rho_4)$	±0.000
$\delta(\sigma_3)$	±0.013
$\delta(\sigma_4)$	±0.000
$\delta(f_B)$	$^{+0.004}_{-0.003}$
$\delta(\mu_1)$	$^{+0.000}_{-0.013}$
$\delta(\mu_0)$	$^{+0.000}_{-0.006}$
$\delta(m_b)$	$^{+0.000}_{-0.001}$
$\delta(m_c)$	±0.000
$\delta(\alpha_s)$	±0.002
δ(CKM)	±0.006

Table G.9 Individual errors for the ratio $\tau(D^+)/\tau(D^0)$ in the PS mass scheme

Parameter	Error contribution
$\delta(\overline{B}_1)$	$^{+0.07}_{-0.05}$
$\delta(\overline{B}_2)$	± 0.00
$\delta(\overline{\epsilon}_1)$	$^{+0.52}_{-0.47}$
$\delta(\overline{\epsilon}_2)$	± 0.017
$\delta(\rho_3)$	± 0.05
$\delta(\rho_4)$	± 0.00
$\delta(\sigma_3)$	± 0.46
$\delta(\sigma_4)$	± 0.00
$\delta(f_D)$	± 0.08
$\delta(\mu_1)$	$^{+0.07}_{-0.40}$
$\delta(\mu_0)$	$^{+0.08}_{-0.21}$
$\delta(m_c)$	± 0.08
$\delta(m_s)$	± 0.00
$\delta(\alpha_s)$	$^{+0.07}_{-0.06}$
δ(CKM)	± 0.00

References

1. Gamiz E, Shigemitsu J, Trottier H (2008) Four fermion operator matching with NRQCD heavy and AsqTad light quarks. Phys Rev D 77:114505. https://doi.org/10.1103/PhysRevD.77.114505, arXiv:0804.1557
2. Monahan C, Gámiz E, Horgan R, Shigemitsu J (2014) Matching lattice and continuum four-fermion operators with nonrelativistic QCD and highly improved staggered quarks. Phys Rev D 90:054015. https://doi.org/10.1103/PhysRevD.90.054015, arXiv:1407.4040
3. Buchalla G (1997) Renormalization of $\Delta B = 2$ transitions in the static limit beyond leading logarithms. Phys Lett B 395:364–368. https://doi.org/10.1016/S0370-2693(97)00043-9, arXiv:hep-ph/9608232
4. Beneke M, Buchalla G, Greub C, Lenz A, Nierste U (2002) The B^+-B_d^0 lifetime difference beyond leading logarithms. Nucl Phys B 639:389–407. https://doi.org/10.1016/S0550-3213(02)00561-8, arXiv:hep-ph/0202106
5. Ciuchini M, Franco E, Lubicz V, Martinelli G, Scimemi I, Silvestrini L (1998) Next-to-leading order QCD corrections to $\Delta F = 2$ effective Hamiltonians. Nucl Phys B 523:501–525. https://doi.org/10.1016/S0550-3213(98)00161-8, arXiv:hep-ph/9711402
6. Buras AJ, Misiak M, Urban J (2000) Two loop QCD anomalous dimensions of flavor changing four quark operators within and beyond the standard model. Nucl Phys B 586:397–426. https://doi.org/10.1016/S0550-3213(00)00437-5, arXiv:hep-ph/0005183
7. Neubert M, Sachrajda CT (1997) Spectator effects in inclusive decays of beauty hadrons. Nucl Phys B 483:339–370. https://doi.org/10.1016/S0550-3213(96)00559-7, arXiv:hep-ph/9603202
8. Ciuchini M, Franco E, Lubicz V, Mescia F (2002) Next-to-leading order QCD corrections to spectator effects in lifetimes of beauty hadrons. Nucl Phys B 625:211–238. https://doi.org/10.1016/S0550-3213(02)00006-8, arXiv:hep-ph/0110375

9. Beneke M, Maier A, Piclum J, Rauh T (2015) The bottom-quark mass from non-relativistic sum rules at NNNLO. Nucl Phys B 891:42–72. https://doi.org/10.1016/j.nuclphysb.2014.12.001, arXiv:1411.3132
10. Beneke M, Maier A, Piclum J, Rauh T (2016) NNNLO determination of the bottom-quark mass from non-relativistic sum rules. In: PoS RADCOR2015, p 035. https://doi.org/10.22323/1.235.0035, arXiv:1601.02949
11. Particle Data Group collaboration, Patrignani C et al (2016) Review of Particle Physics. Chin Phys C 40:100001. https://doi.org/10.1088/1674-1137/40/10/100001
12. Alberti A, Gambino P, Healey KJ, Nandi S (2015) Precision determination of the Cabibbo-Kobayashi-Maskawa element V_{cb}. Phys Rev Lett 114:061802. https://doi.org/10.1103/PhysRevLett.114.061802, arXiv:1411.6560
13. Chetyrkin KG, Kuhn JH, Maier A, Maierhofer P, Marquard P, Steinhauser M et al (2009) Charm and bottom quark masses: an update. Phys Rev D 80:074010. https://doi.org/10.1103/PhysRevD.80.074010, arXiv:0907.2110
14. Wang Z-G (2015) Analysis of the masses and decay constants of the heavy-light mesons with QCD sum rules. Eur Phys J C 75:427. https://doi.org/10.1140/epjc/s10052-015-3653-9, arXiv:1506.01993
15. Gelhausen P, Khodjamirian A, Pivovarov AA, Rosenthal D (2013) Decay constants of heavy-light vector mesons from QCD sum rules. Phys Rev D 88:014015. https://doi.org/10.1103/PhysRevD.88.014015, https://doi.org/10.1103/PhysRevD.91.099901, https://doi.org/10.1103/PhysRevD.89.099901, arXiv:1305.5432
16. Narison S (2013) A fresh look into $m_{c,b}$ and precise $f_{D_{(s)},B_{(s)}}$ from heavy-light QCD spectral sum rules. Phys Lett B 718:1321–1333. https://doi.org/10.1016/j.physletb.2012.10.057, arXiv:1209.2023
17. Lucha W, Melikhov D, Simula S (2011) OPE, charm-quark mass, and decay constants of D and D_s mesons from QCD sum rules. Phys Lett B 701:82–88. https://doi.org/10.1016/j.physletb.2011.05.031, arXiv:1101.5986

Appendix H
Additional Information from "One Constraint to Kill Them All?"

In this appendix, we break down our updated SM calculation in Chap. 7 by showing the inputs used and the resulting error breakdown. We also discuss in more detail the dependence of ΔM_s on inputs from lattice QCD and the CKM matrix elements.

H.1 Numerical Input for Theory Predictions

The inputs we use in our numerical evaluations are shown in Table H.1. The values are taken from the PDG [1, 2], from non-relativistic sum rules (NRSR) [3, 4], from the CKMfitter group [5] and the non-perturbative parameters from FLAG (July 2017 online update [6]). For α_s we use RunDec [7] with 5-loop accuracy [8–12], running from M_Z down to the bottom mass scale. At the low scale we use 2-loop accuracy to determine $\Lambda^{(5)}$.

H.2 Error Budget of the Theory Predictions

In this section we compare the error budget of our new SM prediction for ΔM_s^{SM} with the ones given in 2015 by [13], in 2011 by [14] and 2006 by [15]—the results are shown in Table H.2.

We observe a considerable improvement in accuracy and a sizeable shift compared to the 2015 prediction, mostly stemming from the new lattice results for $f_{B_s}\sqrt{B}$, which is still responsible for the largest error contribution of about 6%. The next important uncertainty is the accuracy of the CKM element V_{cb}, which contributes about 2 % to the error budget. The CKM parameters were determined assuming unitarity of the 3×3 CKM matrix—if this assumption is relaxed, then the uncertainties can increase. The uncertainties due to the remaining parameters are subleading. In

M. J. Kirk, *Charming New Physics in Beautiful Processes?*,
Springer Theses, https://doi.org/10.1007/978-3-030-19197-9

Table H.1 Input parameters for our update of ΔM_s

Parameter	Value	Source
M_{B_s}	$(5.366\,89 \pm 0.000\,19)$GeV	PDG 2017
m_t	(173.1 ± 0.6)GeV	PDG 2017
$\bar{m}_t(\bar{m}_t)$	(165.65 ± 0.57)GeV	Own evaluation
$\bar{m}_b(\bar{m}_b)$	(4.203 ± 0.025)GeV	NRSR
$\alpha_s(M_Z)$	0.1181(11)	PDG 2017
$\alpha_s(\overline{m}_b)$	0.2246(21)	Own evaluation
$\Lambda^{(5)}$	(0.2259 ± 0.0068)GeV	Own evaluation
V_{us}	$0.22508^{+0.00030}_{-0.00028}$	CKMfitter
V_{cb}	$0.04181^{+0.00028}_{-0.00060}$	CKMfitter
$\lvert V_{ub}/V_{cb}\rvert$	0.0889(14)	CKMfitter
γ_{CKM}	$1.141^{+0.017}_{-0.020}$	CKMfitter
$f_{B_s}\sqrt{\hat{B}}$	(274 ± 8)MeV	FLAG

Table H.2 Individual contributions to the theoretical error of the mass difference ΔM_s within the SM and comparison with the values obtained in [13–15]. In the last row the errors are summed in quadrature

Parameter	Error contribution			
	This work (%)	ABL 2015 [13] (%)	LN 2011 [14] (%)	LN 2006 [15] (%)
$\delta(f_{B_s}\sqrt{B})$	5.8	13.9	13.5	34.1
$\delta(\lvert V_{cb}\rvert)$	2.1	4.9	3.4	4.9
$\delta(m_t)$	0.7	0.7	1.1	1.8
$\delta(\alpha_s)$	0.1	0.1	0.4	2
$\delta(\gamma_{\mathrm{CKM}})$	0.1	0.1	0.3	1
$\delta(\lvert V_{ub}/V_{cb}\rvert)$	<0.1	0.1	0.2	0.5
$\delta(\bar{m}_b)$	<0.1	<0.1	0.1	—
$\sum\delta$	6.2	14.8	14.0	34.6

total we are left with an overall uncertainty of about 6%, in comparison to the experimental uncertainty of about 0.1%.

H.3 Non-perturbative Inputs

As a word of caution we present in Table H.3 a wider range of non-perturbative determinations of the matrix elements of the four-quark operators alongside the corresponding predictions for the mass difference.

Table H.3 Predictions for the non-perturbative parameter $f_{B_s}\sqrt{\hat{B}}$ and the corresponding SM prediction for ΔM_s. The current FLAG average is dominated by the FERMILAB/MILC value from 2016. Note that the HQET-SR result is found by combining our result for the bag parameter (Eq. 6.4.2, which was published in [22]) with a separate sum rule calculation of the decay constant

Source	$f_{B_s}\sqrt{\hat{B}}$ (MeV)	$\Delta M_s^{\mathrm{SM}}(\mathrm{ps}^{-1})$
HPQCD14 [16]	(247 ± 12)	(16.2 ± 1.7)
ETMC13 [17]	(262 ± 10)	(18.3 ± 1.5)
HPQCD09 [18] = FLAG13 [19]	(266 ± 18)	(18.9 ± 2.6)
FLAG17[20]	(274 ± 8)	(20.01 ± 1.25)
Fermilab16 [21]	(274.6 ± 8.8)	(20.1 ± 1.5)
HQET-SR [22, 23]	$\left(278^{+28}_{-24}\right)$	$\left(20.6^{+4.4}_{-3.4}\right)$
HPQCD06 [24]	(281 ± 20)	(21.0 ± 3.0)
RBC/UKQCD14 [25]	(290 ± 20)	(22.4 ± 3.4)
Fermilab11 [26]	(291 ± 18)	(22.6 ± 2.8)

HPQCD presented in 2014 preliminary results for $N_f = 2 + 1$ [16]—for our numerical estimate in Table H.3 we extracted the numbers from Fig. 7.3 in those proceedings. When finalised, this new calculation will supersede the 2006 [24] and 2009 [18] values. The ETMC $N_f = 2$ number stems from 2013 [17], it is obtained with only two active flavours in the lattice simulation. The Fermilab/MILC $N_f = 2 + 1$ number is from 2016 [21] and it supersedes the 2011 value [26]. This value currently dominates the FLAG average. The numerical effect of these new inputs on mixing observables was partially studied in Chap. 3. The previous FLAG average from 2013 [19] was considerably lower. There is also a large $N_f = 2 + 1$ value from RBC-UKQCD presented at LATTICE 2015 (update of [25]). However, this number is obtained in the static limit and currently missing $1/m_b$ corrections are expected to be very sizeable.[3] The HQET sum rules estimate for the bag parameter from Chap. 6 can also be combined with the decay constant from lattice.

It would be very desirable to see a convergence of these determinations, and in particular an independent confirmation of the Fermilab/MILC result which currently dominates the FLAG average.

H.4 CKM-Dependence

The second most important input parameter for the prediction of ΔM_s is the CKM parameter V_{cb}. There is a long-standing discrepancy between the inclusive determination and values obtained from studying exclusive B decays, see [27]. Recent studies

[3] Private communication with Tomomi Ishikawa.

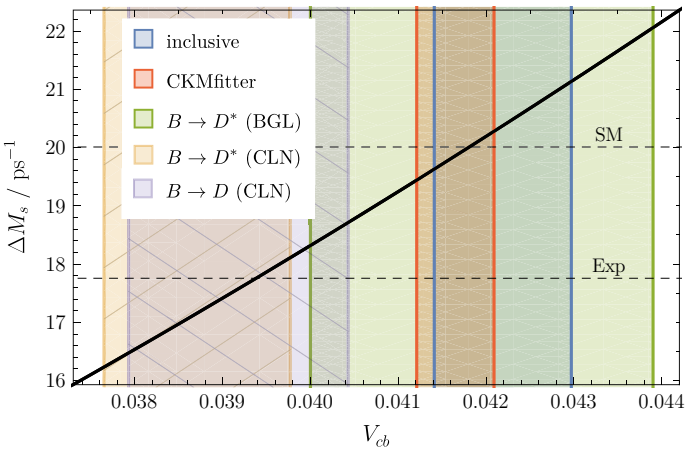

Fig. H.1 Dependence of the SM prediction of ΔM_s on the value of V_{cb}

have found that a problem with the use of a certain form factor parameterisation in the experimental analysis might be the cause of the low exclusive value. The form factor models are denoted by CLN [28] and BGL [29]. Traditionally experiments had used CLN, but it appears that this might underestimate some uncertainties. Using the BGL parameterisation instead one finds (see [30–33]) values that lie considerably closer to the inclusive one. Currently, there are various determinations of V_{cb} available:

$$
\begin{aligned}
V_{cb}^{\text{Inclusive}} &= 0.04219 \pm 0.00078\,[34] \\
V_{cb}^{B\to D} &= 0.03918 \pm 0.00094 \pm 0.00031\,[34] \\
V_{cb}^{B\to D^*,\,\text{CLN}} &= 0.03871 \pm 0.00047 \pm 0.00059\,[34] \\
V_{cb}^{B\to D^*,\,\text{BGL}} &= 0.0419^{+0.0020}_{-0.0019}\,[30]\,.
\end{aligned}
$$

In Fig. H.1 we plot the dependence of the SM prediction of ΔM_s on V_{cb}, and show the regions predicted by the above inclusive and exclusive determinations. We use the CKMfitter result for V_{cb} (see Table H.1) for our new SM prediction of ΔM_s (see Eq. 7.2.3 and the (upper) horizontal dashed line denoted with "SM"), and the corresponding error band is shown in orange. The predictions obtained by using the inclusive value of V_{cb} only are given by the blue region. For completeness we also show the regions obtained by using the various exclusive extractions of V_{cb}. The disfavoured CLN values result in much lower values for the mass difference (hatched areas), while the BGL value agrees well with the inclusive region, albeit with a higher uncertainty. The experimental value of ΔM_s is shown by the (lower) horizontal dashed line denoted with "Exp".

The preference for the inclusive determination agrees with the value obtained from the CKM fit (which we use in our SM estimate), as well as with the fit value

that is found if the direct measurements of V_{cb} are not included in the fit [5]:

$$V_{cb}^{\text{CKMfitter (no direct)}} = 0.04235^{+0.00074}_{-0.00069}\,. \tag{H.4.1}$$

We also note that the CKMfitter determinations take into account loop-mediated processes, where potentially NP could be present and affect the determination. Taking only tree-level inputs, they find[4]:

$$|V_{us}| = 0.22520^{+0.00012}_{-0.00038}\,, \tag{H.4.2}$$

$$|V_{cb}| = 0.04175^{+0.00033}_{-0.00172}\,, \tag{H.4.3}$$

$$|V_{ub}/V_{cb}| = 0.092^{+0.004}_{-0.005}\,, \tag{H.4.4}$$

$$\gamma_{\text{CKM}} = 1.223^{+0.017}_{-0.030}\,, \tag{H.4.5}$$

and using these inputs we find

$$\Delta M_s^{\text{SM,2017 (tree)}} = 19.9 \pm 1.5\text{ps}^{-1}\,, \tag{H.4.6}$$

which shows an overall consistency with the prediction in Eq. 7.2.3.

References

1. Particle Data Group collaboration, Patrignani C et al (2016) Review of Particle Physics. Chin Phys C 40:100001. https://doi.org/10.1088/1674-1137/40/10/100001
2. Particle Data Group collaboration. http://pdg.lbl.gov/
3. Beneke M, Maier A, Piclum J, Rauh T (2015) The bottom-quark mass from non-relativistic sum rules at NNNLO. Nucl Phys B 891:42–72. https://doi.org/10.1016/j.nuclphysb.2014.12.001, arXiv:1411.3132
4. Beneke M, Maier A, Piclum J, Rauh T (2016) NNNLO determination of the bottom-quark mass from non-relativistic sum rules. In: PoS RADCOR2015, p 035. https://doi.org/10.22323/1.235.0035. arXiv:1601.02949
5. CKMfitter collaboration, ICHEP 2016 results. http://ckmfitter.in2p3.fr/www/results/plots_ichep16/num/ckmEval_results_ichep16.html
6. FLAG collaboration. http://flag.unibe.ch/MainPage
7. Herren F, Steinhauser M (2018) Version 3 of RunDec and CRunDec. Comput Phys Commun 224:333–345. https://doi.org/10.1016/j.cpc.2017.11.014, arXiv:1703.03751
8. Baikov PA, Chetyrkin KG, Kühn JH (2017) Five-loop running of the QCD coupling constant. Phys Rev Lett 118:082002. https://doi.org/10.1103/PhysRevLett.118.082002, arXiv:1606.08659
9. Herzog F, Ruijl B, Ueda T, Vermaseren JAM, Vogt A (2017) The five-loop beta function of Yang-Mills theory with fermions. JHEP 02:090. https://doi.org/10.1007/JHEP02(2017)090, arXiv:1701.01404
10. Luthe T, Maier A, Marquard P, Schroder Y (2017) Complete renormalization of QCD at five loops. JHEP 03:020. https://doi.org/10.1007/JHEP03(2017)020, arXiv:1701.07068
11. Luthe T, Maier A, Marquard P, Schroder Y (2017) The five-loop Beta function for a general gauge group and anomalous dimensions beyond Feynman gauge. JHEP 10:166. https://doi.org/10.1007/JHEP10(2017)166, arXiv:1709.07718

[4] Private communication with Sébastien Descotes-Genon.

12. Chetyrkin KG, Falcioni G, Herzog F, Vermaseren JAM (2017) Five-loop renormalisation of QCD in covariant gauges. JHEP 10:179 . https://doi.org/10.1007/JHEP12(2017)006, https://doi.org/10.3204/PUBDB-2018-02123, https://doi.org/10.1007/JHEP10(2017)179, arXiv:1709.08541
13. Artuso M, Borissov G, Lenz A (2016) CP violation in the B_s^0 system. Rev Mod Phys 88:045002. https://doi.org/10.1103/RevModPhys.88.045002, arXiv:1511.09466
14. Lenz A, Nierste U (2011) Numerical updates of lifetimes and mixing parameters of B mesons. In: CKM unitarity triangle. Proceedings, 6th international workshop, CKM 2010, Warwick, UK, Sept 6–10, 2010. arXiv:1102.4274, http://inspirehep.net/record/890169/files/arXiv:1102.4274.pdf
15. Lenz A, Nierste U (2007) Theoretical update of $B_s - \bar{B}_s$ mixing. JHEP 06:072. https://doi.org/10.1088/1126-6708/2007/06/072, arXiv:hep-ph/0612167
16. Dowdall RJ, Davies CTH, Horgan RR, Lepage GP, Monahan CJ, Shigemitsu J, B-meson mixing from full lattice QCD with physical u, d, s and c quarks. arXiv:1411.6989
17. ETM collaboration, Carrasco N et al (2014) B-physics from $N_f = 2$ tmQCD: the standard model and beyond. JHEP 03:016. https://doi.org/10.1007/JHEP03(2014)016, arXiv:1308.1851
18. HPQCD collaboration, Gamiz E, Davies CTH, Lepage GP, Shigemitsu J, Wingate M (2009) Neutral B Meson Mixing in Unquenched Lattice QCD. Phys Rev D 80:014503. https://doi.org/10.1103/PhysRevD.80.014503, arXiv:0902.1815
19. Aoki S et al (2014) Review of lattice results concerning low-energy particle physics. Eur Phys J C 74:2890. https://doi.org/10.1140/epjc/s10052-014-2890-7, arXiv:1310.8555
20. Aoki S et al (2017) Review of lattice results concerning low-energy particle physics. Eur Phys J C 77:112. https://doi.org/10.1140/epjc/s10052-016-4509-7, arXiv:1607.00299
21. Fermilab Lattice, MILC collaboration, Bazavov A et al (2016) $B_{(s)}^0$-mixing matrix elements from lattice QCD for the standard model and beyond. Phys Rev D 93:113016. https://doi.org/10.1103/PhysRevD.93.113016, arXiv:1602.03560
22. Kirk M, Lenz A, Rauh T (2017) Dimension-six matrix elements for meson mixing and lifetimes from sum rules. JHEP 12:068. https://doi.org/10.1007/JHEP12(2017)068, arXiv:1711.02100
23. Gelhausen P, Khodjamirian A, Pivovarov AA, Rosenthal D (2013) Decay constants of heavy-light vector mesons from QCD sum rules. Phys Rev D 88:014015. https://doi.org/10.1103/PhysRevD.88.014015, https://doi.org/10.1103/PhysRevD.91.099901, https://doi.org/10.1103/PhysRevD.89.099901, arXiv:1305.5432
24. Dalgic E, Gray A, Gamiz E, Davies CTH, Lepage GP, Shigemitsu J et al (2007) $B_s^0 - \bar{B}_s^0$ mixing parameters from unquenched lattice QCD. Phys Rev D 76:011501. https://doi.org/10.1103/PhysRevD.76.011501, arXiv:hep-lat/0610104
25. Aoki Y, Ishikawa T, Izubuchi T, Lehner C, Soni A (2015) Neutral B meson mixings and B meson decay constants with static heavy and domain-wall light quarks. Phys Rev D 91:114505. https://doi.org/10.1103/PhysRevD.91.114505, arXiv:1406.6192
26. Bouchard CM, Freeland ED, Bernard C, El-Khadra AX, Gamiz E, Kronfeld AS et al (2011) Neutral B mixing from $2 + 1$ flavor lattice-QCD: the standard model and beyond. In: PoS LATTICE2011, p 274. https://doi.org/10.22323/1.139.0274, arXiv:1112.5642
27. Particle Data Group collaboration, Semileptonic B-hadron decays, determination of V_{cb}, V_{ub}. http://pdg.lbl.gov/2017/reviews/rpp2017-rev-vcb-vub.pdf
28. Caprini I, Lellouch L, Neubert M (1998) Dispersive bounds on the shape of anti-B $\to$ D(*) lepton anti-neutrino form-factors. Nucl Phys B 530:153–181. https://doi.org/10.1016/S0550-3213(98)00350-2, arXiv:hep-ph/9712417
29. Boyd CG, Grinstein B, Lebed RF (1995) Constraints on form-factors for exclusive semileptonic heavy to light meson decays. Phys Rev Lett 74:4603–4606. https://doi.org/10.1103/PhysRevLett.74.4603, arXiv:hep-ph/9412324
30. Grinstein B, Kobach A (2017) Model-independent extraction of $|V_{cb}|$ from $\bar{B} \to D^* \ell \overline{\nu}$. Phys Lett B 771:359–364. https://doi.org/10.1016/j.physletb.2017.05.078, arXiv:1703.08170

31. Bigi D, Gambino P, Schacht S (2017) $R(D^*)$, $|V_{cb}|$, and the Heavy Quark Symmetry relations between form factors. JHEP 11:061. https://doi.org/10.1007/JHEP11(2017)061, arXiv:1707.09509
32. Bernlochner FU, Ligeti Z, Papucci M, Robinson DJ (2017) Tensions and correlations in $|V_{cb}|$ determinations. Phys Rev D 96:091503. https://doi.org/10.1103/PhysRevD.96.091503, arXiv:1708.07134
33. Jaiswal S, Nandi S, Patra SK (2017) Extraction of $|V_{cb}|$ from $B \to D^{(*)}\ell\nu_\ell$ and the standard model predictions of $R(D^{(*)})$. JHEP 12:060. https://doi.org/10.1007/JHEP12(2017)060, arXiv:1707.09977
34. HFLAV collaboration, Amhis Y et al (2017) Averages of b-hadron, c-hadron, and τ-lepton properties as of summer 2016. Eur Phys J C 77:895. https://doi.org/10.1140/epjc/s10052-017-5058-4, arXiv:1612.07233